ABSTRACT

HEAT TRANSFER IN SILICON – EXPERIMENTS AND SIMULATION

by
Chihlin Huang

The purpose of this thesis is to study the heat transfer in silicon. Silicon is the key semiconductor material, and thermal processing is the traditional method that is used in semiconductor processing. In this research, we can predict the temperature of the silicon wafer during heating. This ability to predict wafer temperature during semiconductor processing will facilitate in the following: (a) Process temperature uniformity, (b) Film thickness uniformity, (c) Diffusion, (d) Process yield, (e) Thermally induced stresses, and (f) Device yield – spatially and temporally across the wafer. For low temperature applications, IC chips can be modeled to simulate the heat flow. Therefore, the status of the chip while heating can be studied to understand the influence of the heating process on the performance of the chips, which is useful in the assessment of device performance and reliability.

The research, in this thesis, utilizes a traditional hot plate as the source of heating of the silicon wafer. The modeling of heating of the wafer is based on ANSYS CFX software, a software tool that permits to solve fluid flow problems. The model considers heat conduction in silicon wafer, heat convection in air, and heat radiation. The influence of silicon wafer thickness and diameter on the wafer temperature distribution is simulated.

HEAT TRANSFER IN SILICON – EXPERIMENTS AND SIMULATION

by
Chihlin Huang

A Thesis
Submitted to the Faculty of
New Jersey Institute of Technology
in Partial Fulfillment of the Requirement for the Degree of
Master of Science in Materials Science and Engineering

Interdisciplinary Program in Materials Science and Engineering

January 2017

Blank Page

APPROVAL PAGE

HEAT TRANSFER IN SILICON - EXPERIMENTS AND SIMULATION

Chihlin Huang

Dr. Nuggehalli M. Ravindra, Thesis Advisor Date
Professor, Department of Physics

Dr. Michael Jaffe, Research Professor Date
Department of Biomedical Engineering, NJIT

Dr. Eon Soo Lee, Assistant Professor Date
Department of Mechanical and Industrial Engineering, NJIT

BIOGRAPHICAL SKETCH

Author: Chihlin Huang

Degree: Master of Science

Date: January 2017

Undergraduate and Graduate Education:

- Master of Science in Materials Science and Engineering
  New Jersey Institute of Technology, Newark, NJ, 2017

- Bachelor of Science in Physics
  National Central University, Taoyuan, Taiwan, 2008

Major: Materials Science and Engineering

To my dear family and friends.

獻給我最親愛的家人

ACKNOWLEDGEGEMENT

I thank my thesis adviser Dr. N.M. Ravindra, for his constant guidance and encouragement. Special thanks to my committee members, Prof. Michael Jaffe and Prof. Eon Soo Lee for their support.

Also, I am very grateful for the help and support from my parents throughout my life.

TABLE OF CONTENTS

TABLE OF CONTENTS
(Continued)

TABLE OF CONTENTS
(Continued)

LIST OF TABLES

LIST OF TABLES
(Continued)

LIST OF FIGURES

LIST OF FIGURES
(Continued)

LIST OF FIGURES
(Continued)

CHAPTER 1

INTRODUCTION

In semiconductor manufacturing processes, the wafer temperature is a significant parameter. The temperature affects several processes. These processes include the following:

In photolithography, temperature affects the quality and hardness of the photoresists.

In APCVD, LPCVD, and PECVD, temperature is a significant factor to form SiNx thin films.

In epitaxy, temperature plays an important role for the GaN growth process.

In diffusion process, for applications in silicon integrated circuit technology, the temperature range is in between 950 to 1100 °C.

Rapid thermal processing (RTP) is used in a variety of process applications in the temperature range of 800 to 1150°C.

The most frequently used heating methods are furnaces and rapid thermal processors (RTP), and the most commonly used temperature monitoring methods in semiconductor manufacturing are thermocouples and pyrometers. A summary of the various semiconductor process steps and the associated temperature ranges are summarized in Table 1.1.

Table 1.1 Working Temperatures for Semiconductor Processes

Semiconductor Process		Working Temperature(°C)	Source
Photolithography	AZP400 Photoresists Baking	110	[1]
	Su-8 Photoresists Baking	95	[2]
APCVD	SiNx Layers	700-900	[3]
LPCVD	SiNx Layers	750	[3]
PECVD	SiNx Layers	below 500	[3]
MOCVD	GaN growth	1050	[4]
RTP	Silicon diffusion	850-1050	[5]

The goal of this research is to simulate the temperature distribution on silicon wafer during heating of the wafer. ANSYS CFX software, a modeling tool that has been applied to solve fluid flow problems, was chosen to address the problem. This model contains heat conduction in silicon wafer, heat convection in air, and heat radiation. The construction of the model considers the silicon wafer thickness and the wafer diameter as input parameters to determine the temperature distribution across the wafer.

In Chapter 2, the fundamentals of heat transfer of silicon are discussed. In Chapter 3, the properties of silicon are introduced. In Chapter 4, the heat transfer in silicon is presented. In Chapter 5, the temperature measurement techniques are explored, for example: thermocouples, pyrometers, IR camera and thermography. In Chapter 6, experimental details and results are discussed. In Chapter 7, approaches to modeling heat transfer is demonstrated. In Chapter 8, discussions of the simulation results are presented. Chapter 9, the last chapter in this thesis, focuses on conclusions and future directions.

CHAPTER 2

FUNDAMENTALS OF HEAT TRANSFER

Heat transfer is the process in which heat moves from one location in a material to another location within the material or across the material. The three methods of heat transfer are conduction, convection, and radiation.

2.1 Heat Conduction

2.1.1 Introduction to Heat Conduction

Heat conduction is the process in which heat is transferred by the vibration of particles within an object at high temperature to a location within the object at a low temperature. The thermal conductivity is a material dependent property.

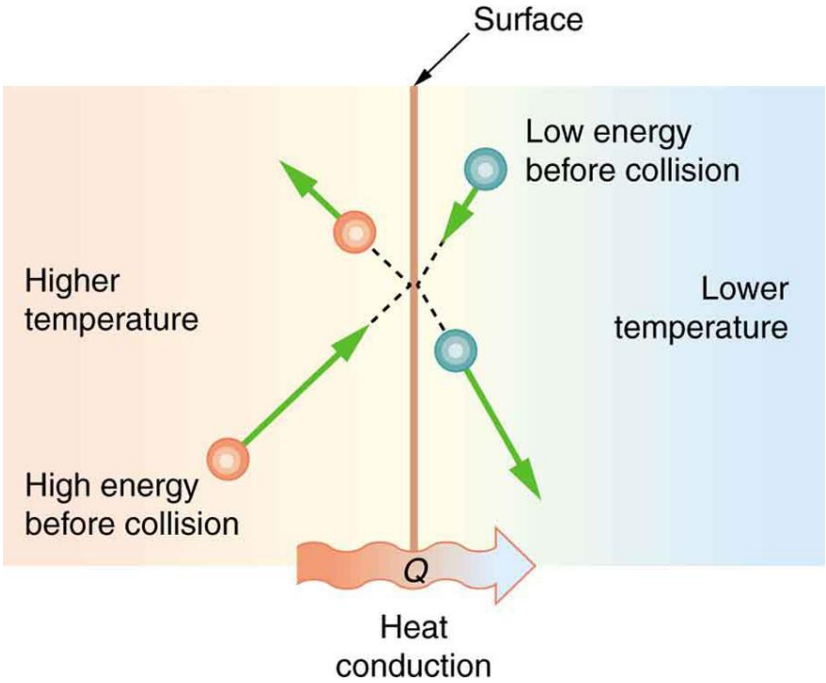

Figure 2.1 Illustration of heat conduction.

Source: http://cdn.phys.org/newman/gfx/news/hires/2014/whatisheatco.jpg

2.1.2 Fourier's Law

Fourier's law, also known as the law of heat conduction, describes that in a unit time, the volume of heat transfer through a substance to another is inversely proportional to the temperature change.

$$q = -k\nabla u \tag{2.1}$$

where q is the heat flux density ($W \cdot m^{-2}$), k is the thermal conductivity of the material, and ∇u is the gradient of temperature ($K \cdot m^{-1}$). In common materials, the thermal conductivity of a material, k, is usually a constant. However, it varies with temperature in some cases.

In three-dimensional form, Equation (2.1) becomes

$$q = -k\nabla u \cdot \hat{n} \tag{2.2}$$

2.1.3 Heat Equation

The heat equation can be derived by Fourier's law and the principle of conservation of energy [6]. The heat flux, through the boundary S of the sub-region V, is the normal component of the heat flux vector q, $q \cdot \hat{n}$, where $\hat{n}$ is the outward unit normal at the boundary S (Figure 2.2).

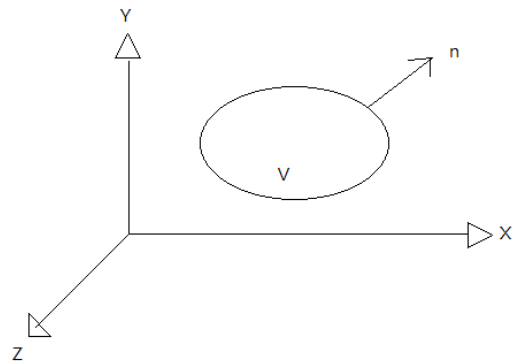

Figure 2.2 The heat flux through the boundary S of the sub-region V.

Conservation of energy implies that the rate of change of heat energy equals heat energy into V from boundaries per unit time plus heat energy generated in solid per unit time. The conservation of energy principle leads to the following:

$$\frac{d}{dt}\int_V c\rho u \, dV = -\int_S q \cdot \hat{n} \cdot dS + \int_V F \cdot dV \tag{2.3}$$

From Gauss'sTheorem, Equation (2.3) becomes:

$$\frac{d}{dt}\int_V c\rho u \, dV = -\int_V \nabla \cdot q \, dV + \int_V F \, dV \tag{2.4}$$

Since V is independent of time, Equation (2.4) can be written as:

$$\int_V \left(c\rho \frac{\partial u}{\partial t} + \nabla q - F \right) dV = 0 \tag{2.5}$$

The integrand must be zero everywhere; so Equation (2.5) becomes:

$$c\rho \frac{\partial u}{\partial t} + \nabla q - F = 0 \tag{2.6}$$

Using equation (2.2), assuming k as a constant, Equation (2.6) becomes:

$$c\rho \frac{\partial u}{\partial t} - k\nabla^2 u = F \tag{2.7}$$

In Cartesian coordinates, Equation (2.7) can be presented as:

$$c\rho \frac{\partial u}{\partial t} - \left[\frac{\partial}{\partial t}(ku_x) + \frac{\partial}{\partial x}\left(ku_y\right) + \frac{\partial}{\partial t}(ku_z)\right] = F(x, y, z, t) \tag{2.8}$$

where u is temperature, c is the specific heat capacity, ρ is the mass density. In addition, Equation (2.8) can be expressed as thermal diffusivity $\alpha = \sqrt{\frac{k}{c\rho}}$

$$\frac{\partial u}{\partial t} = a^2 \nabla^2 u + f\left(x, y, z, t\right) \tag{2.9}$$

2.1.4 Thermal Contact Resistance

Generally, when two materials are in contact with each other, we assume that the surfaces that are in contact with each other have the same temperature as the interface. However, the temperatures on the two surfaces are not the same. There is a heat loss due to the gaps that occur between contacting surfaces. These gaps create contact resistance, contributing to additional thermal resistance, which is called thermal contact resistance[7]. The thermal contact resistance can be expressed by the following equation:

$$R_c = \frac{\Delta T}{Q_{contact} + Q_{gap}} (m^2 {}^\circ C/W) \tag{2.10}$$

where R_c is the thermal contact resistance, ΔT is the temperature difference between surfaces, $Q_{contact}$ is the heat loss through contact, Q_{gap} is the heat absorbed by the gap.

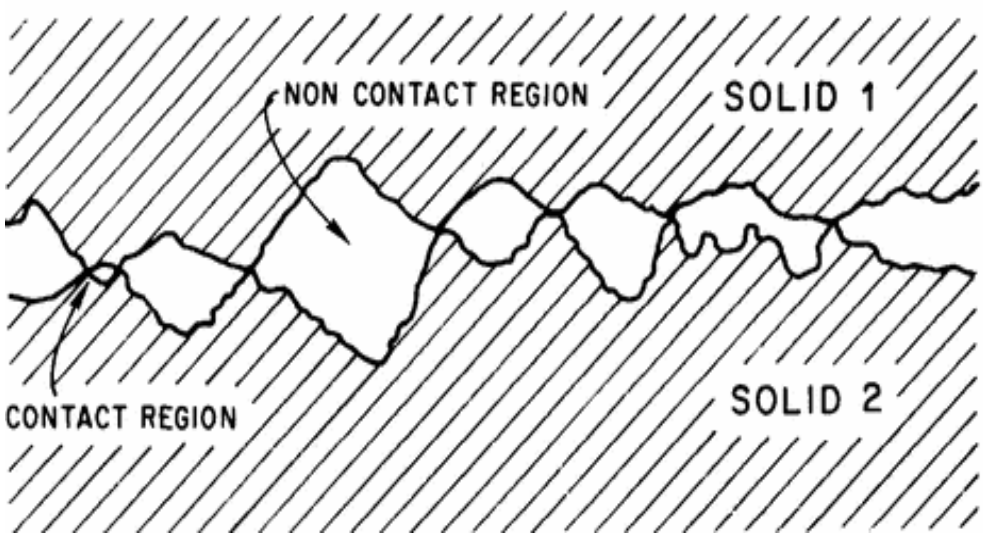

Figure 2.3 Illustration of a contact interface.
Source:[8]

2.2 Heat Convection

2.2.1 Introduction to Heat Convection

Heat convection is heat transfer when groups of molecules move within fluids. It follows the Newton's law of cooling.

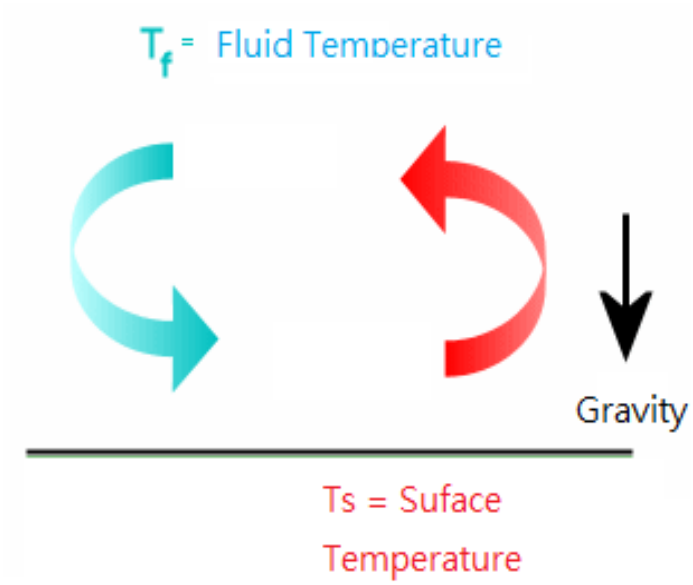

Figure 2.4 Illustration of heat convection

2.2.2 Newton's Law of Cooling

The equation to Newton's law of cooling is given by:

$$q_{convection} = h\ A\ (T_s - T_f) \tag{2.12}$$

where, $q_{convection}$ is the heat transferred per unit (W), A is the area of the object (m^2), h is the heat transfer coefficient (W/ m^2K), T_s is the object's surface temperature (K), and T_f is the fluid temperature (K)

2.3 Thermal Radiation

2.3.1 Introduction to Thermal Radiation

Thermal radiation is the electromagnetic radiation emitted by bodies because of its temperature. Unlike the heat conduction and the heat convection, thermal radiation does not require medium to transfer heat.

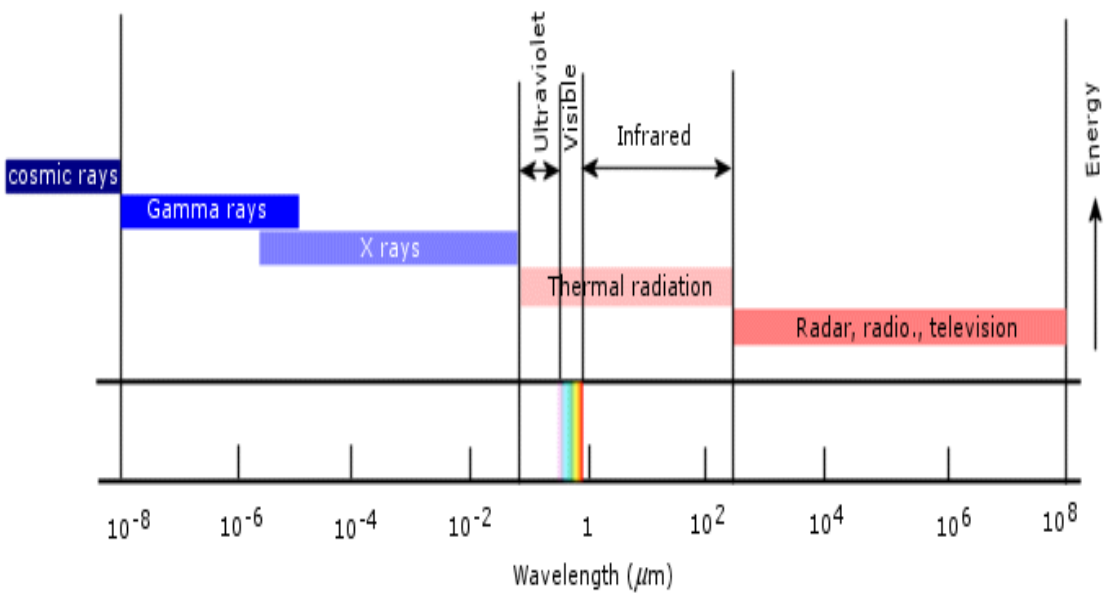

Figure 2.5 Bands of electromagnetic spectrum at their respective wavelengths.
Source: http://help.solidworks.com/

2.3.2 Energy Exchange in Surface

When radiated photons reach another surface, they may be absorbed, reflected, or transmitted. Their relationship can be presented by the following equation:

$$\alpha + \rho + \tau = 1 \tag{2.13}$$

where, α is absorptance, ρ is reflectance, and τ is transmittance.

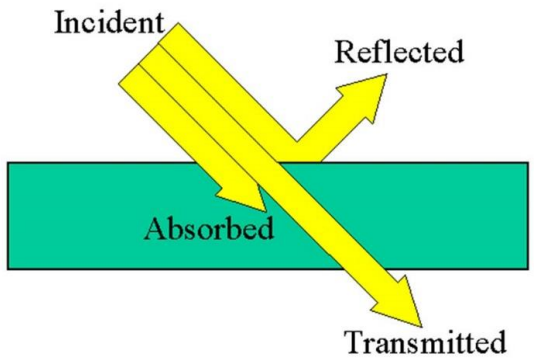

Figure 2.6 Radiated photons are absorbed, reflected, or transmitted by the surface.
Source: https://etorgerson.wordpress.com/

Absorptance, or absorption coefficient, depending on the material, is how effective the material can absorb radiant energy, and it is the fraction of incident radiation absorbed. Absorption of electromagnetic radiation is the way that materials take up the energy from photons. Absorptance can be represented by the equation:

$$\alpha = \frac{4\pi\kappa}{\lambda} \tag{2.14}$$

where, κ is extinction coefficient, and λ is the wavelength of heat radiation

Reflection is when a wave enters from a medium to another, and it returns to the original medium. Reflectance is the fraction of incident radiation reflected, and can be described by the equation (2.15):

$$\rho = \frac{(n-1)^2 + \kappa^2}{(n+1)^2 + \kappa^2} \tag{2.15}$$

where, n is the refractive index and κ is the extinction coefficient.

Transmittance is how effective the material transmits radiant energy, and it is the fraction of incident radiation transmitted. Transmittance is related to the absorption coefficient [9] by:

$$\tau = \exp(-\alpha t) \tag{2.16}$$

where, α is the absorption coefficient, t is the thickness of the material.

Transparency, translucency and opacity can be defined by absorptance, reflectance and transmittance. An opaque material has no transmission; Transparency allows radiation to totally pass through the body; Translucent material allows radiation to pass through but loses some of it. Black body absorbs and emits all of the radiation. Table 2.1 summarizes each kind of material relative to its absorptance, reflectance, and transmittance.

Table 2.1 Materials can be Classified Based on Their Absorptance, Reflectance and Transmittance

<table>
<tr><th></th><th>Opaque Body</th><th>Transparent Body</th><th>Translucent Body</th><th>Black Body</th></tr>
<tr><td>τ</td><td>0</td><td>1</td><td>$0<\tau<1$</td><td>0</td></tr>
<tr><td>α</td><td rowspan="2">$\alpha+\rho=1$</td><td>0</td><td rowspan="2">$0<\alpha+\rho<1$</td><td>1</td></tr>
<tr><td>ρ</td><td>0</td><td>0</td></tr>
</table>

2.3.3 Thermal Radiation Power

Planck's law represents the electromagnetic radiation emitted by a black body in proportion to the black body temperature[10].

$$w_\lambda = \frac{2\pi hc^2}{\lambda^5} x \frac{1}{e^{\frac{hc}{\lambda k_B T}} - 1} \tag{2.17}$$

where, w_λ is blackbody radiant emittance, λ is Wavelength (μm), h is Planck's constant (6.6×10^{-34} joule.s), c is the velocity of light in vacuum (3×10^{6} m/s), k_B is Boltzmann's constant (1.4×10^{-23} joule/K), and T is temperature (K).

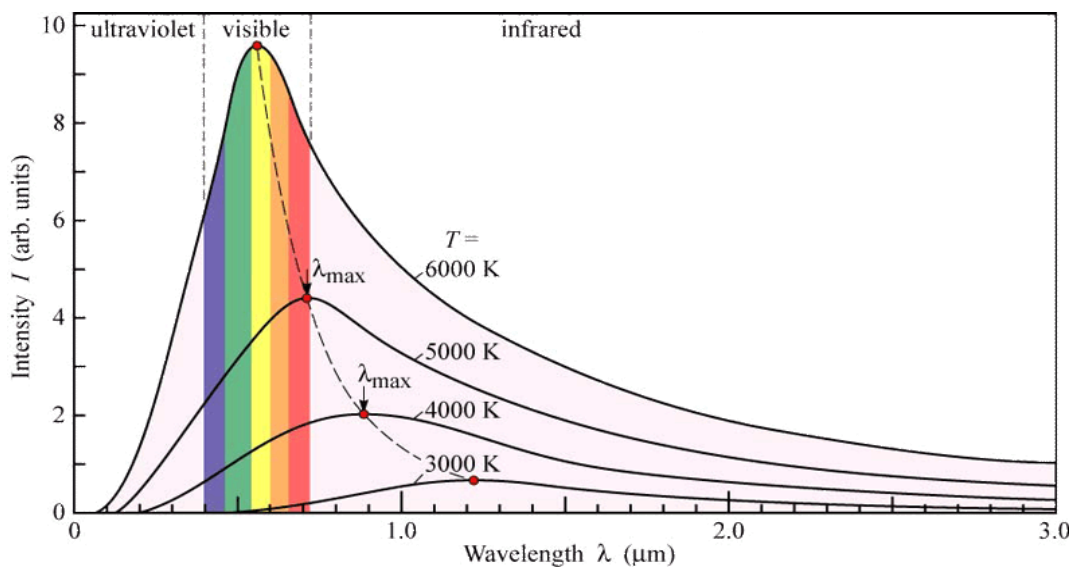

Figure 2.7 Curves of Black Body spectral radiation, which refers to Planck's distribution.
Source: https://onwardtotheedge.wordpress.com/

Stefan's law is an expression for the total power per unit area radiated at all wavelengths; therefore, it is the result of integrating the Planck's formula from λ=0 to λ=∞:

$$W = \sigma T_1^4 \tag{2.18}$$

where, W is the total radiant emittance of a black body, T is the object's temperature, ε (0 < ε < 1) is emissivity and σ is the Stefan-Boltzmann constant or Stefan's constant.

$$\sigma = \frac{2\pi^5 {k_B}^4}{15c^2h^3} = 5.670373 \ \text{x} \ 10^{-8} Wm^{-2}K^{-4} \tag{2.19}$$

2.3.4 Emissivity

Since most of the materials do not act like a black body, a factor, Emissivity, is introduced. Under the same circumstance, Emissivity is defined as the ratio of the energy radiated from a material's surface to the energy radiated from a blackbody. The volume of emissivity is between 0 (for a opaque body) and 1 (for a black body). The formula (2.18) becomes (2.20) [11]:

$$W = \varepsilon\sigma T_1^4 \tag{2.20}$$

The emissivity depends not only on the material itself but also on the feature of the surface. For example, the emissivity of a polished aluminum surface is 0.02, but the emissivity for an oxidized aluminum surface is 0.3. Table 2.2 lists emissivity for some common materials.

Table 2.2 Emissivity of Common Materials

Emissivity of Materials					
Material	Feature	Emissivity	Material	Feature	Emissivity
Aluminum	Oxidized	3	Marble		0.94
	Polished	0.020-0.4			
Asbestos		0.95	Mortar		0.89-0.91
Asphalt		0.95	Oil		0.94
Brass	Oxidized	0.5	Paper		0.95
	Polished	0.02-0.05			
Brick		0.9-0.96	Plaster		0.8-0.9
Carbon		0.85	Plastic	Non-transparent	0.95
Cement		0.96	Plastic cement	0.85-0.95	
Ceramics		0.95	Rock		0.7
Charcoal	Powdered	0.96	Rubber		0.95
Clay		0.92-0.96	Sand		0.9
Concrete		0.95	Snow		0.83-0.9
Glass		0.85-0.92	Soap Bubble		0.75-0.8
Gold		0.01-0.1	Soil		0.9-0.98
Graphite	Oxidized	0.2-0.6	Steel	Oxidized	0.7-0.9
Human Skin		0.98	Textile		0.9
Ice		0.96-0.98	Wood		0.9-0.95
Iron	Oxidized	0.7			

source: Lasergrip 1022 Non-Contact Inferred Thermometer User Manual.

CHAPTER 3

PROPERTIES OF SILICON

3.1 Introduction

Silicon is the 14th element in the periodic table, and it exhibits the diamond lattice structure in a single crystal form (Figure 3.1). Some properties of silicon are as follows: The atomic density of silicon is 5 x 10^{22} atoms/$cm^{3,}$ and the atomic weight is 28.09u (1u = 1.66054 x 10^{-27}kg). The density of silicon is 2.328 g/$cm^{3.}$ The conduction electron mobility in lightly doped silicon is 1350 cm^2/V, while that of hole mobility is 475 cm^2/V at 300K. The shear stress for silicon is 3.61 x 107 dyne/cm^2. The detailed properties are listed below in Table 3.1.

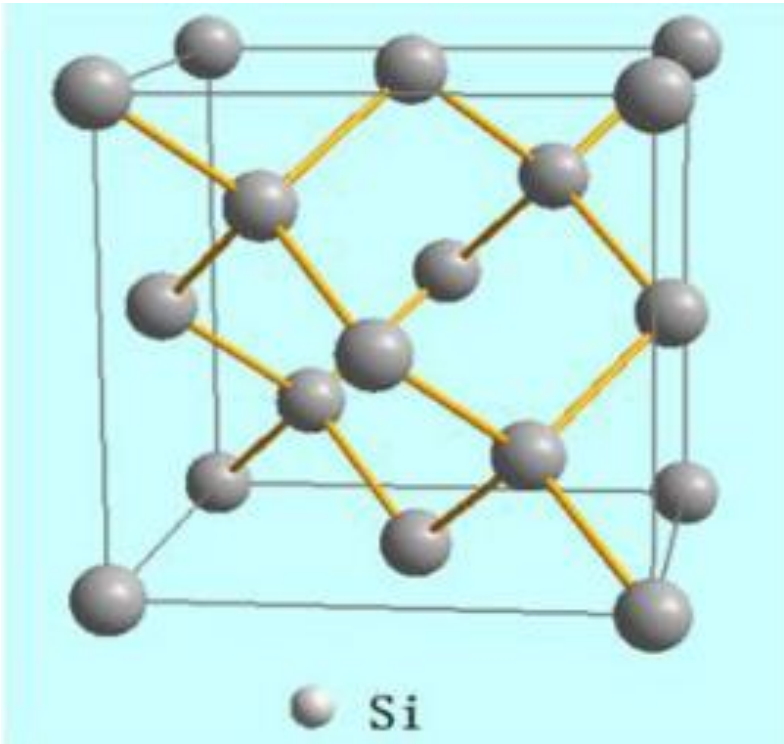

Figure 3.1 The crystalline structure of silicon

Source:[12]

Table 3.1 Properties of Silicon

Properties of Silicon	
Crystal Structure	Diamond
Lattice constant (Å)	5.0×10^{22}
Atoms/cm^3	5.0×10^{22}
Atomic weight	28.09
Density (g/cm^3)	2.328
Minority carrier lifetime (s)	2.5×10^{-3}
Electrical/Optical Properties	
Dielectric constant	11.9
Effective density of States in conduction band, N_c (cm^{-3})	2.8×10^{19}
Effective density of States in valence band, N_v (cm^{-3})	1.04×10^{19}
Effective Mass, m^*/m_0 Electrons	$m_l^* = 0.98$
	$m_t^* = 0.19$
Effective Mass, m^*/m_0 Holes	$m_l\ h^* = 0.16$
	$m_h\ h^* = 0.49$
Electron affinity, χ(V)	4.05
Energy gap (eV) at 300K	1.12
Intrinsic carrier concentration (cm^{-3})	1.45×10^{10}
Intrinsic Debye length (μm)	24
Intrinsic resistivity (Ω-cm)	2.3×10^5
Electrical/Optical Properties	
Mobility (drift) (cm^2/V-s)	1500 450
Optical-phonon energy (eV)	0.063
Phonon mean free path λ_0 (Å)	76(electron) 55(hole)
Thermal Properties	
Melting point (ºC)	1415
Linear coefficient of thermal expansion, $\Delta L/L\Delta T$ (ºC^{-1})	2.6×10^{-6}
Specific heat (J/g ºC)	0.7
Thermal conductivity at 300 K (W/cm ºC)	1.5
Thermal diffusivity (cm^2/s)	0.9
Vapor pressure (Pa)	1 at 1650 ºC 10^{-6} at 900 ºC

Source: [13]

3.2 Semiconductors

Semiconductors are materials that have a resistivity between insulators, which have a high resistivity, and metals, which have a high conductivity

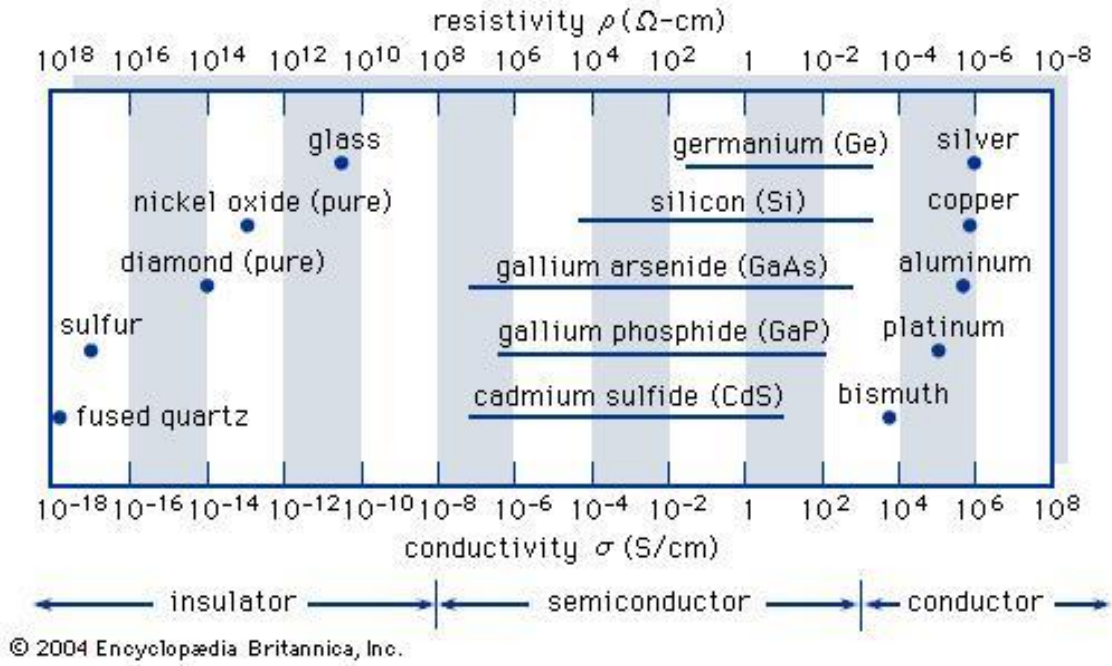

Figure 3.2 Conductivity/resistivity for insulators/semiconductors/conductors.
source: https://media1.britannica.com/eb-media/07/207-004-2B66F205.jpg

Silicon is the most common material used in semiconductor manufacturing. The reasons that silicon has been chosen as the semiconductor material are as follows:

(a) Silicon is cheap and inexhaustible since the earth's crust contains 26.3% of silicon in any form.

(b) Silicon has an indirect band-gap (1.17 eV), and this prevents its applications in photonics although investigations in this area continue.

(c) Silicon is very inexpensive and offers a naturally occurring dielectric in the form of SiO_2 which is very stable and reliable. This has led to silicon based integrated circuits and thus VLSI/MOS technology dominates the applications of silicon.

(d) In the area of solar cells, silicon is a major player since its theoretical conversion efficiency and experimentally obtained conversion efficiency have begun to converge.

(e) Silicon, in the wafer form and in the device form, is highly scalable and reliable. The manufacturing of Silicon-based microprocessors has demonstrated yields of 99% in manufacturing.

(f) The extraction and purification methods of silicon from its raw material are effective.

Table 3.2 Semiconductors in Periodic Table.

II	III	IV	V	VI
	Al Aluminum	Si Silicon	P Phosphorous	S Sulfur
Zn Zinc	Ga Gallium	Ge Germanium	As Arsenic	Se Selenium
Cd Cadmium	In Indium	Sn Tin	Sb Antimony	Te Tellurium
Hg Mercury				

source: http://ezphysics.nchu.edu.tw/

3.2.1 Doping

Doping is the method to change the electrical properties of semiconductors. It is done by adding impurity to the intrinsic (pure) semiconductor in order to increase its electrical conductivity. The doped semiconductors are known as extrinsic semiconductors. The

common extrinsic semiconductors are categorized into p-type semiconductors and n-type semiconductors.

The formation of an n-type semiconductor requires that pentavalent atoms (such as arsenic, phosphorus, antimony) are added to tetravalent atoms (for example, silicon). For example, in Figure 3.3, a phosphorous atom and four surrounded silicon atoms form a crystal structure**.** Four phosphorous valence electrons bond with silicon valence electrons, and an extra electron is left, which forms a free electron. Each phosphorous atom produces a free electron in intrinsic Si. Therefore, adding pentavalent atoms produces more free electrons, and increases the electrical conductivity of tetravalent atoms. Since the population density of electrons are more than that of holes, the electrons are majority carriers and the holes are minority carriers.

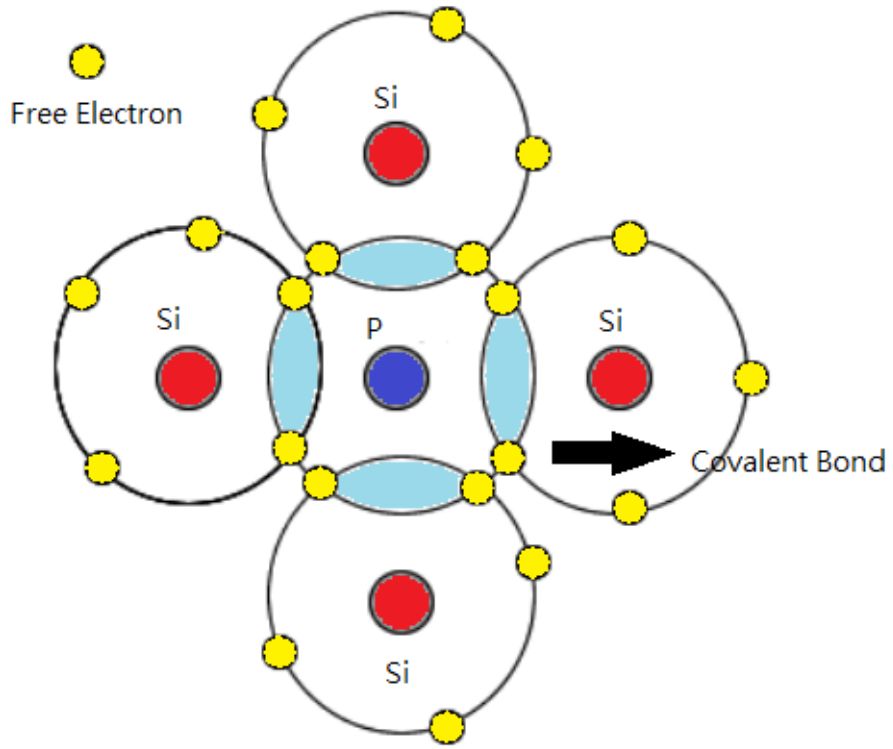

Figure 3.3 Schematic of a typical n-type Semiconductor.

The definition of a p-type semiconductor is that atoms with trivalent electrons (for instance, aluminum, gallium, indium) are added to tetravalent atoms such as silicon. In Figure 3.4, a gallium atom and four surrounded silicon atoms bond with each other into a lattice structure**.** Three electrons from gallium bond with electrons from silicon, and a hole is left. Each gallium atom produces a hole so that adding trivalent atoms to tetravalent atoms produces free holes and increases the electrical conductivity. The holes are majority carriers and the electrons are minority carriers.

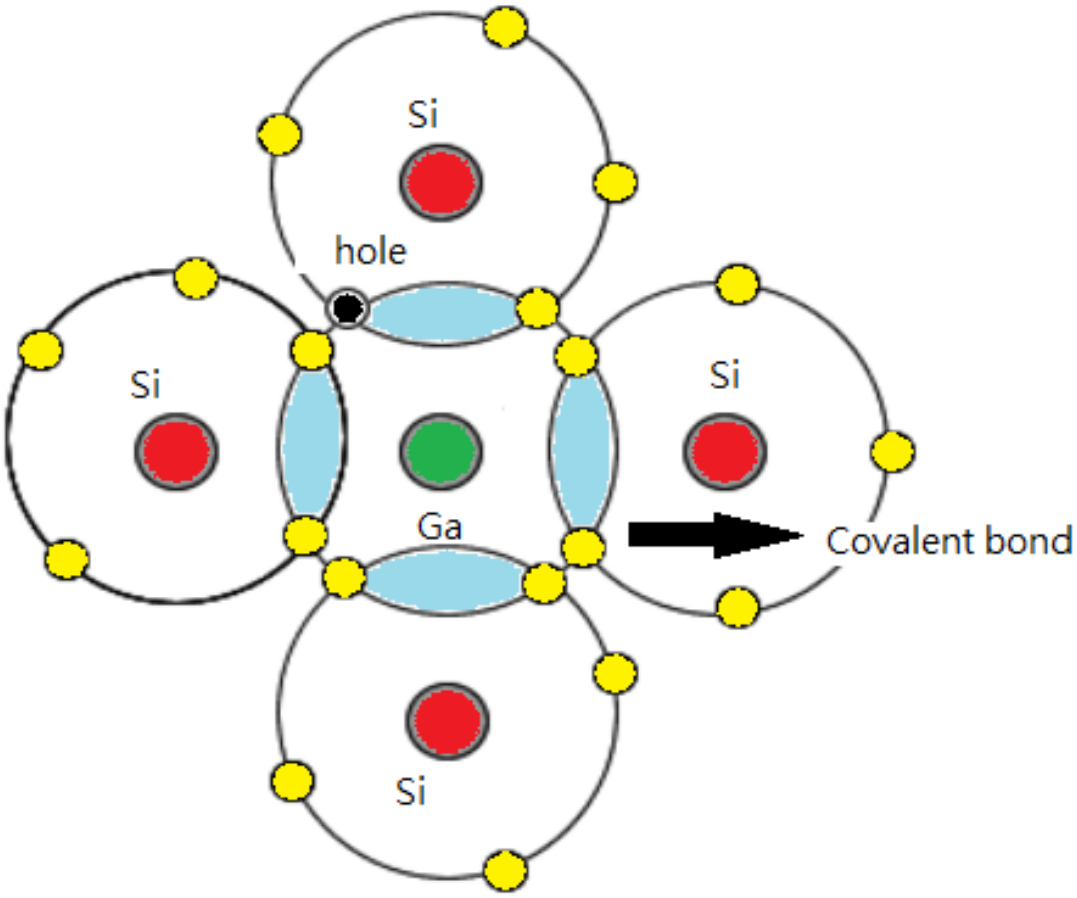

Figure 3.4 Schematic of a typical p-Type Semiconductor.

In intrinsic semiconductor, a hole is left when an electron leaves a covalent bond, which means each electron pairs a hole. Therefore, the concentration of conduction electrons n is equal to the concentration of holes p.

$$n=p=n_i=p_i \tag{3.1}$$

n_i and p_i represent the concentration of conduction electrons and holes in intrinsic semiconductors. They represent intrinsic carrier concentration. For silicon at 300 K,

$$n_i^2 = (n_i \text{ x } p_i) = 2\text{x}10^{20}/\text{cm}^3 \tag{3.2}$$

Table 3.3 Intrinsic Carrier Concentration and Energy Gap of Semiconductors.

Semiconductor	$n_i(\text{cm}^{-3})$	E_g(eV)
Ge	$2.4\text{x}10^{13}$	0.67
Si	$1.45\text{x}10^{10}$	1.12
GaAs	$1.79\text{x}10^{6}$	1.42

For intrinsic semiconductors, n_i depends on the band gap E_g, and the absolute temperature.

$$n_i = n_o \exp\left[-\frac{Eg}{KT}\right] \tag{3.3}$$

Figure 3.5 shows the intrinsic carrier density for Ge, Si, GaAs, and GaP versus temperature.

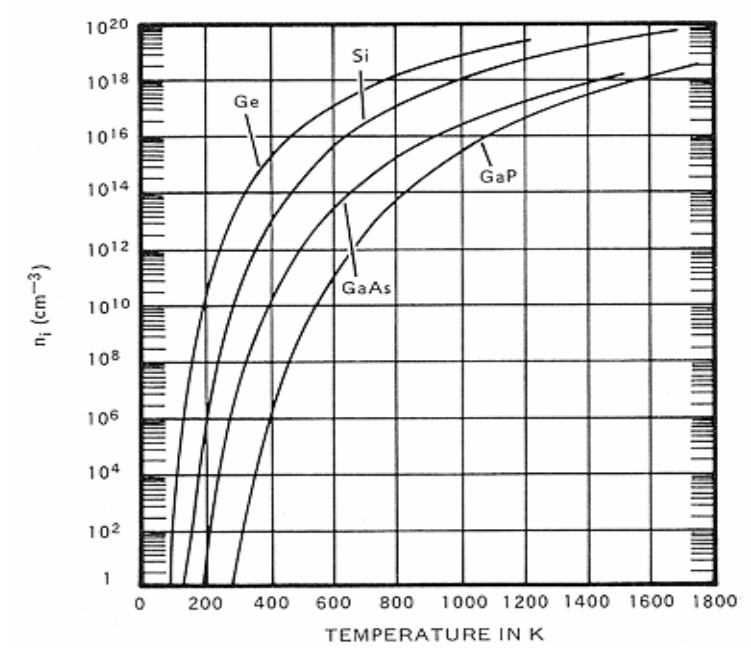

Figure 3.5 Intrinsic carrier density versus temperature.
Source:[14]

3.2.2 Band Gap Theory

The value of the band gap E_g determines if the material is an insulator, metal or semiconductor. In a metal, band gap does not exist since the valence band and conduction band overlap. The band gap in a semiconductor is much smaller than an insulator. A small band gap allows the electrons to excite from the valence band to the conduction band by absorbing the energy.

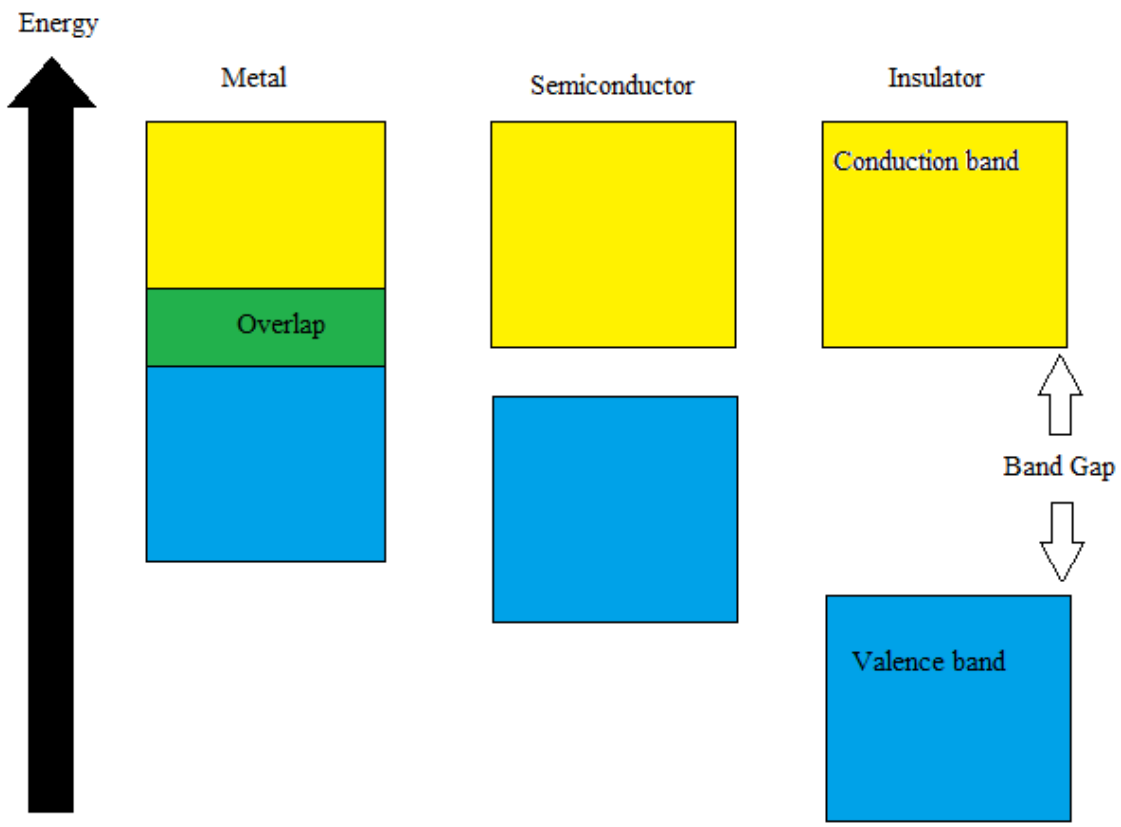

Figure 3.6 Schematic representation of band gaps for a metal, semiconductor and an insulator.

For semiconductors, there are two types of band gaps, direct and indirect energy band gaps. A direct band gap is that the maximum point of the valence band is aligned with the minimum point of the conduction band. An indirect band gap is that the maximum point of the valence band is not aligned with the minimum point of the conduction band.

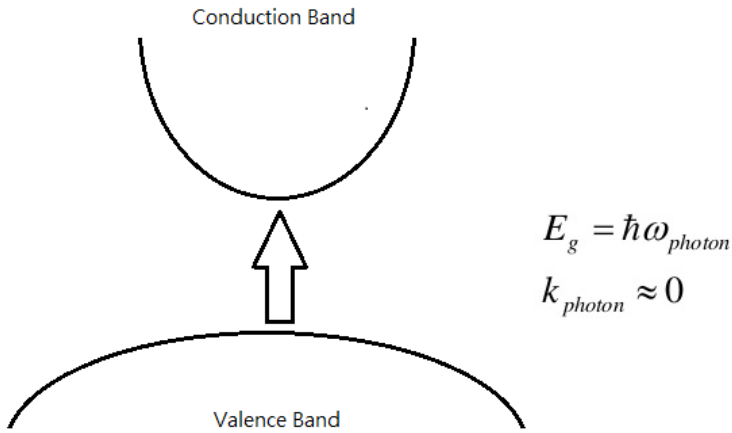

Figure 3.7 Illustration of direct band gap.

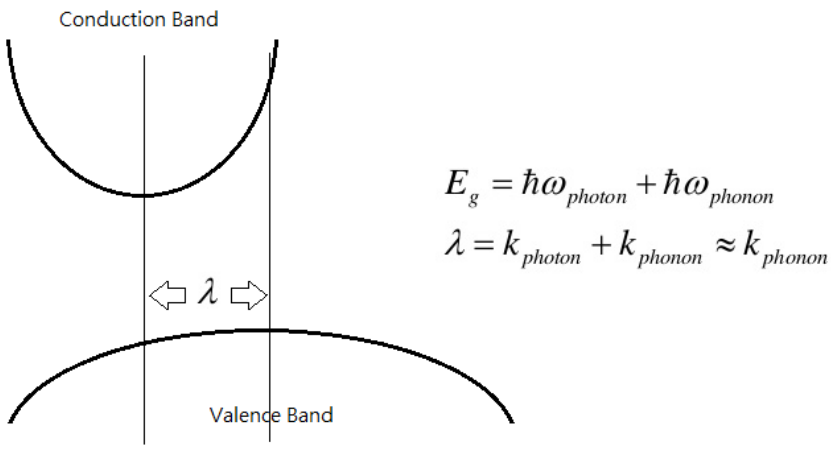

Figure 3.8 Illustration of indirect band gap.

CHAPTER 4

HEAT TRANSFER IN SILICON

4.1 Thermal Properties of Silicon

Some of the common thermal properties of silicon are summarized in Table 4.1. However, some properties change with temperature such as thermal expansion coefficient, thermal conductivity, and thermal diffusivity. These properties will be discussed and expressed as function of temperature in the next section.

Table 4.1 Thermal Properties of Silicon

Melting point (ºC)	1415
Linear coefficient of thermal expansion, $\Delta L/L\Delta T$ (ºC^{-1})	2.6 x 10^{-6}
Specific heat (J/g ºC)	0.7
Thermal conductivity at 300 K (W/cm ºC)	1.48
Thermal diffusivity (cm^2/s)	0.9
Vapor pressure (Pa)	1 at 1650 ºC 10^{-6} at 900 ºC

Source: [13]

4.2 Thermal Diffusivity of Silicon

Thermal diffusivity is a property based on material and is used for calculating unsteady heat conduction. This value represents how quickly a material changes its temperature. The thermal diffusivity must be known in order to calculate and simulate the temperature field since it is a requisite for solving the Heat equation. Thermal diffusivity is proportional to the thermal conductivity.

Table 4.2 Thermal Diffusivity of Silicon versus Temperature

T (K)	D(cm^2 s^{-1})	T(K)	D(cm^2 s^{-1})
50	63.5	400	0.52
60	37.6	500	0.37
70	24.8	600	0.29
80	17.1	700	0.24
90	14.4	800	0.19
100	11.3	900	0.16
150	4.24	1000	0.14
200	2.23	1200	0.12
250	1.23	1400	0.12
300	0.86		

Source:[15]

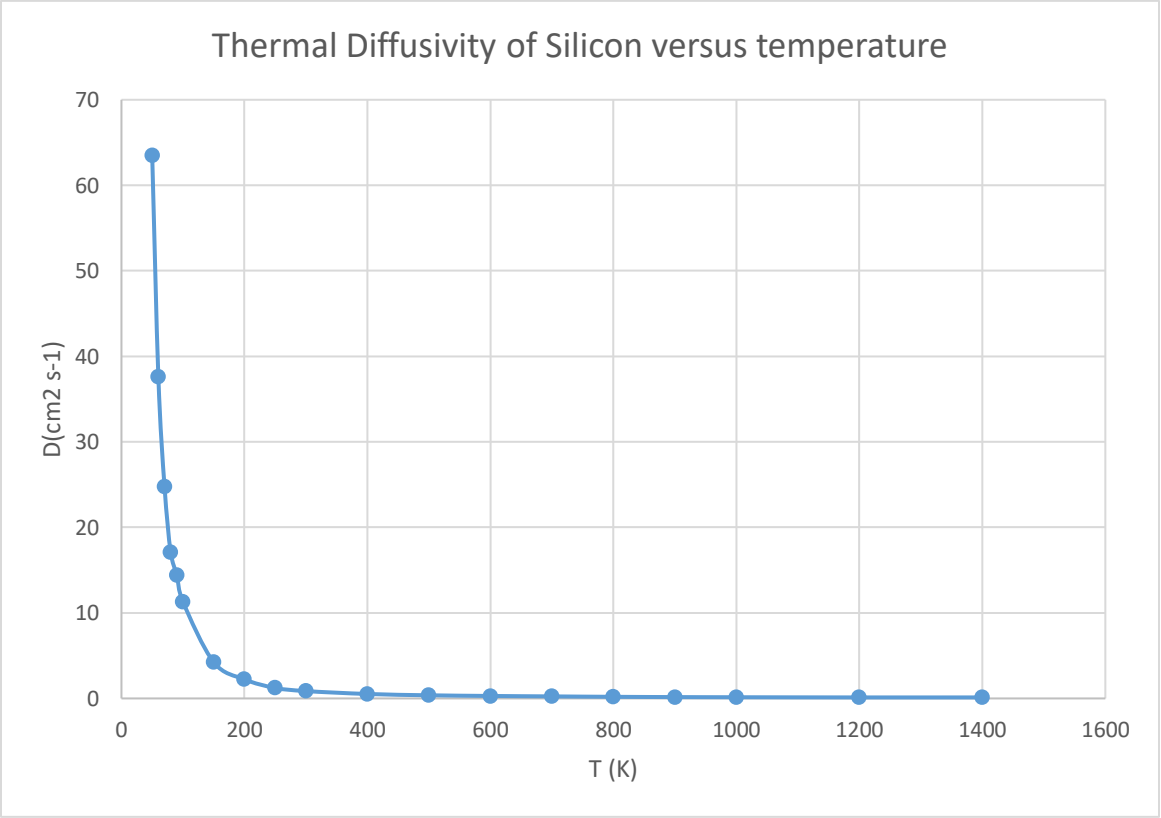

Figure 4.1 Thermal diffusivity of silicon versus temperature.

4.3 Thermal Conductivity of Silicon

Thermal conductivity is a value that represents the ability of a material to change its temperature during heat transfer. The relationship between thermal conductivity and thermal diffusivity is given by the following equation:

$$\alpha = \frac{\lambda}{\rho C_{\rho}} \tag{4.1}$$

where, α is thermal diffusivity, λ is thermal conductivity, ρ is density, and $C\rho$ is specific heat capacity. Figure 4.2 and Table 4.3 show the thermal conductivity of silicon versus temperature at 1 atm. The thermal conductivity of silicon increases rapidly from 1K to 20K, reaches the maximum value of 4160(W/m K), and then swiftly deceases. At 200K, the thermal conductivity decreases slowly.

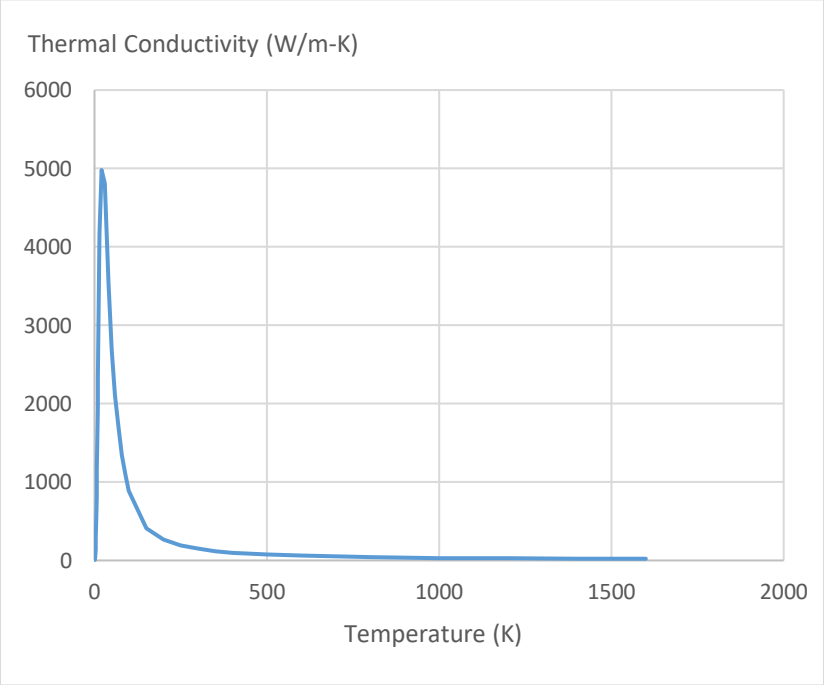

Figure 4.2 Thermal conductivity of silicon versus temperature.

Table 4.3 Thermal Conductivity of Silicon versus Temperature at 1 atm (101.325 kpa)

Temperature (K)	Thermal Conductivity (W/m·K)	Temperature (K)	Thermal Conductivity (W/m·K)
1	6.93	150	409
2	45.4	200	264
3	138	250	191
4	297	300	148
5	527	350	119
6	823	400	98.9
7	1170	500	76.2
8	1550	600	61.9
9	1950	700	52
10	2330	800	42.2
15	4160	900	36
20	4980	1000	31.2
30	4810	1100	28
40	3530	1200	25.7
50	2680	1300	25
60	2110	1400	23.5
70	1680	1500	23
80	1340	1600	22.1
90	1080	1681	22
100	884		

Source : http://www.efunda.com/materials/elements/ , [15],[16],[17]

4.4 Thermal Expansion Coefficient

Thermal expansion coefficient is a material property that is indicative of the extent to which a material expands upon heating. Different substances expand by different amounts. Over small temperature ranges, the thermal expansion of uniform linear objects is proportional to temperature change. Thermal expansion finds useful applications in bimetallic strips for the construction of thermometers but can generate detrimental internal stress when a structural part is heated and kept at constant length.[18]

The thermal expansion of silicon decreases from 0K to 80K. Then, it suddenly increases at the minimum point of 80K, and behaves like a logarithmic function until the temperature has reached the melting point.

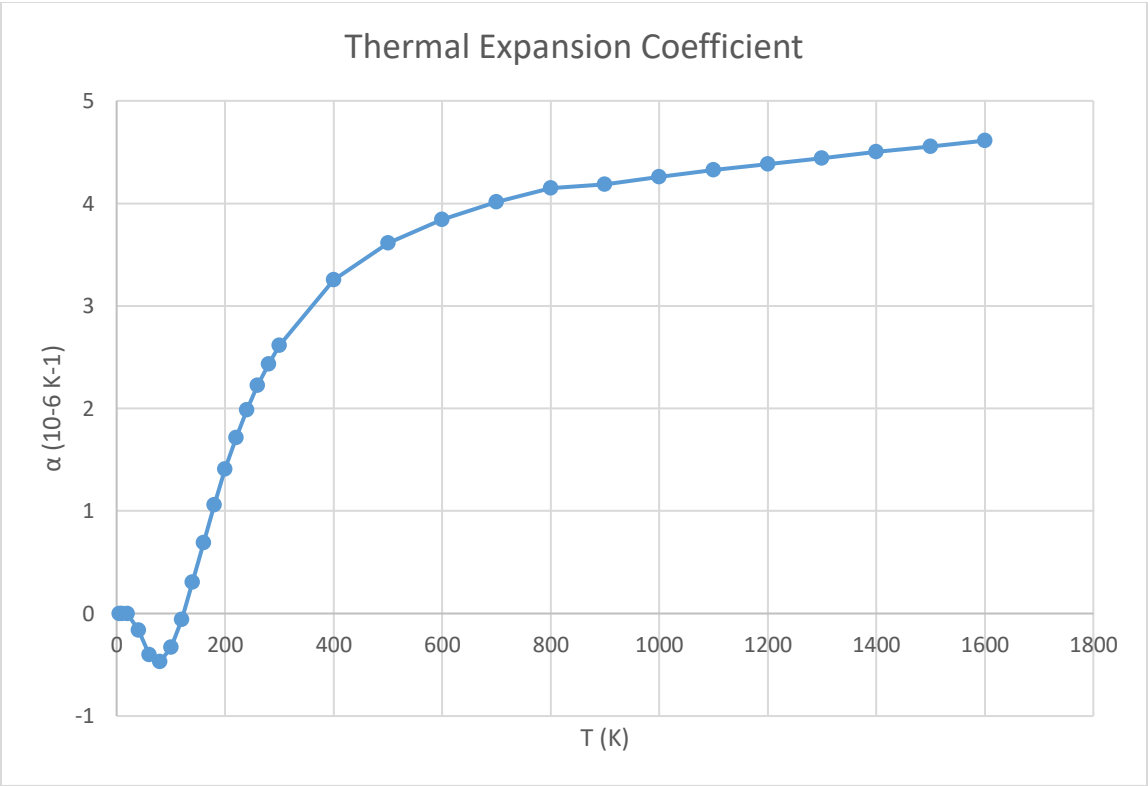

Figure 4.3 Thermal expansion coefficient of silicon versus temperature

Table 4.4 Thermal Expansion Coefficient of Silicon versus Temperature

T (K)	α (10^{-6} K^{-1})	T (K)	α (10^{-6} K^{-1})
5	0.6 x 10^{-4}	280	2.432
10	0.48 x 10^{-3}	300	2.616
20	-0.29 x 10^{-2}	400	3.253
40	-0.164	500	3.614
60	-0.4	600	3.842
80	-0.472	700	4.016
100	-0.33	800	4.151
120	-0.057	900	4.185
140	0.306	1000	4.258
160	0.689	1100	4.323
180	1.061	1200	4.384
200	1.406	1300	4.442
220	1.715	1400	4.5
240	1.986	1500	4.556
260	2.223	1600	4.612

Source: [15],[19]

CHAPTER 5

TEMPERATURE MEASUREMENT TECHNIQUES

Temperature measurement techniques are very useful in fundamental R&D as well as in manufacturing. These include contact methods such as thermocouples, and non-contact methods such as pyrometer, infrared camera, and thermo-reflectance thermography.

Temperature measurement techniques play an important role in semiconductor manufacturing processes. Since the temperature is the factor affecting most of the semiconductor manufacturing processes such as annealing, growth or deposition of films, photo lithography etc., obtaining the accurate temperature of the wafer is one of the most significant tasks. The most commonly used temperature measurement techniques in semiconductor manufacturing processes are thermocouples and optical pyrometers.

5.1 Contact Methods

5.1.1 Thermocouples

In 1821, the German physicist Thomas John Seebeck found that, in a circuit composed of two different metals, if the junction temperature at the two metals is different, the circuit will produce an electro motive force. This phenomenon is known as the thermoelectric effect or the "Seebeck effect".

The thermocouple is an electrical device based on the thermoelectric effect. It is made up of two different metals. When two metals are in contact, at different temperatures, the thermocouple produces a voltage due to the thermoelectric effect. Therefore, the output voltage can be used to measure the temperature.

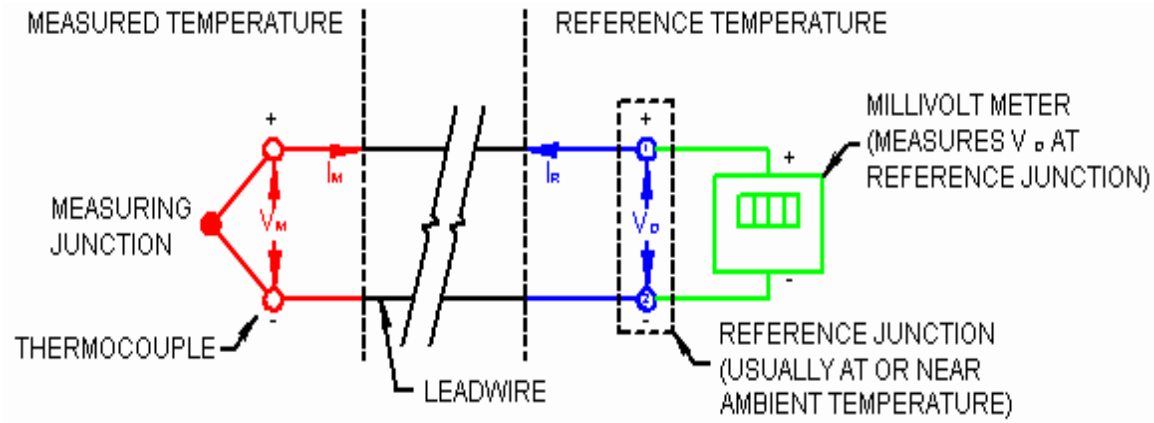

Figure 5.1 A typical thermocouple circuit.

Source: http://claustemp.coman-htp05.htm

Temperature range and sensitivity are the most general requirements for various applications. Different types of thermocouples are made for different applications.

5.1.2 Types of Thermocouples

For commonly used metal combinations, the difference of volts per degree Celsius is between 1 and 70 microvolts per degree Celsius, and some of the metal combinations have become industrial standards. Selection criteria of the combination is decided by availability, chemical properties, cost, melting point, voltage output, and stability.

Standard thermocouple types are listed below.

A type T thermocouple is suitable for cryogenic measurements. The positive thermoelement for a type T thermocouple is copper and the negative thermoelement for a type T thermocouple is 44Ni-55Cu alloy[20].

A Type-J thermocouple is widely used because of its versatility and low cost. It consists of positive thermoelement iron and negative thermoelement 44Ni-55Cu alloy.

In a Type-E thermocouple, the positive thermoelement is 90Ni-9Cr and the negative element is 44Ni-55Cu[20].

Similar to Type-J, a Type-K thermocouple is widely used in industrial applications. For a Type-K thermocouple, the positive thermoelement is 90Ni-9Cr alloy and the negative thermoelement is 94% Ni alloy containing traces of silicon, manganese, aluminum, iron and cobalt[20].

A Type-N thermocouple, Nicrosil/Nisil, was developed for oxidation resistance. Its positive thermoelement is Nicrosil, which contains 14 Cr, 1.4 Si, 0.1 Mg, bal Ni, and its negative thermoelement is Nisil, which contains 4.4 Si, 0.1 Mg, bal Ni[20].

A Type-R thermocouple is very similar to a type S. However, it has a slightly higher emf. It consists of a positive thermoelement, Pt-13Rh and a negative thermoelement, platinum [20].

A Type-S thermocouple consists of the positive thermoelement, Pt-10Rh and the negative thermoelement, high purity platinum. The Type-S thermocouple is widely used in industrial laboratories as a standard for calibration of base-metal thermocouples and other temperature-sensing instruments[20].

A Type-B thermocouple contains a positive thermoelement Pt-30Rh and a negative thermoelement Pt-6Rh. Type-B is less sensitive than Type-R or Type-S, but it can be used in still air or inert atmospheres since its working temperature is up to1700°C [20]. Table 5.1 summarizes the materials used for thermos-elements and their working temperatures.

Table 5.1 Materials used for Thermocouples and Working Temperatures

Type	Thermoelement		Temperature range, °C	
	Positive	Negitive	min	max
T	Copper	44Ni-55Cu	0	350
J	Iron	44Ni-55Cu alloy	0	750
E	90Ni-9Cr	44Ni-55Cu	0	900
K	90Ni-9Cr alloy	94% Ni alloy	0	1250
N	Nicrosil,	Nisil	0	1250
R	Pt-13Rh	Pt	0	1450
S	Pt-10Rh	High purity platinum	0	1450
B	Pt-30Rh	Pt-6Rh	800	1700

5.1.3 Pros and Cons of Thermocouples

Thermocouples are one of the most commonly used temperature sensing devices in the industry. Their advantages are as follows: (a) High measurement accuracy. Thermocouples are directly in contact with the measured object. (b) Wide measurement range. The measurement range for a commonly used thermocouple is from -50℃ to 1600 ℃. Furthermore, some special thermocouples can work at -269℃ or 2800℃. (c) The structure is simple, and it is easy to use.

The cons of thermocouples are as follows: (a) Substantial signal conditioning is required. When measuring microvolt-level signal variations, noise from stray and magnetic fields can be a problem. The measuring device should provide signal filtering. (b) Erosion of metals results in reduced accuracy. Therefore, the thermocouples require careful maintenance.

5.2 Non-Contact Methods

5.2.1 Pyrometers

A pyrometer, which is a non-contact temperature sensor, contains an optical system and a detector. The device measures the amount of heat radiation that is emitted from an object.

5.2.1.1 Optical Pyrometers. An optical pyrometer consists of an outer tube with a red light filter, an absorption screen, and a lens inside, and a circuit that consist of a reference lamp, multi-meters and rheostat.

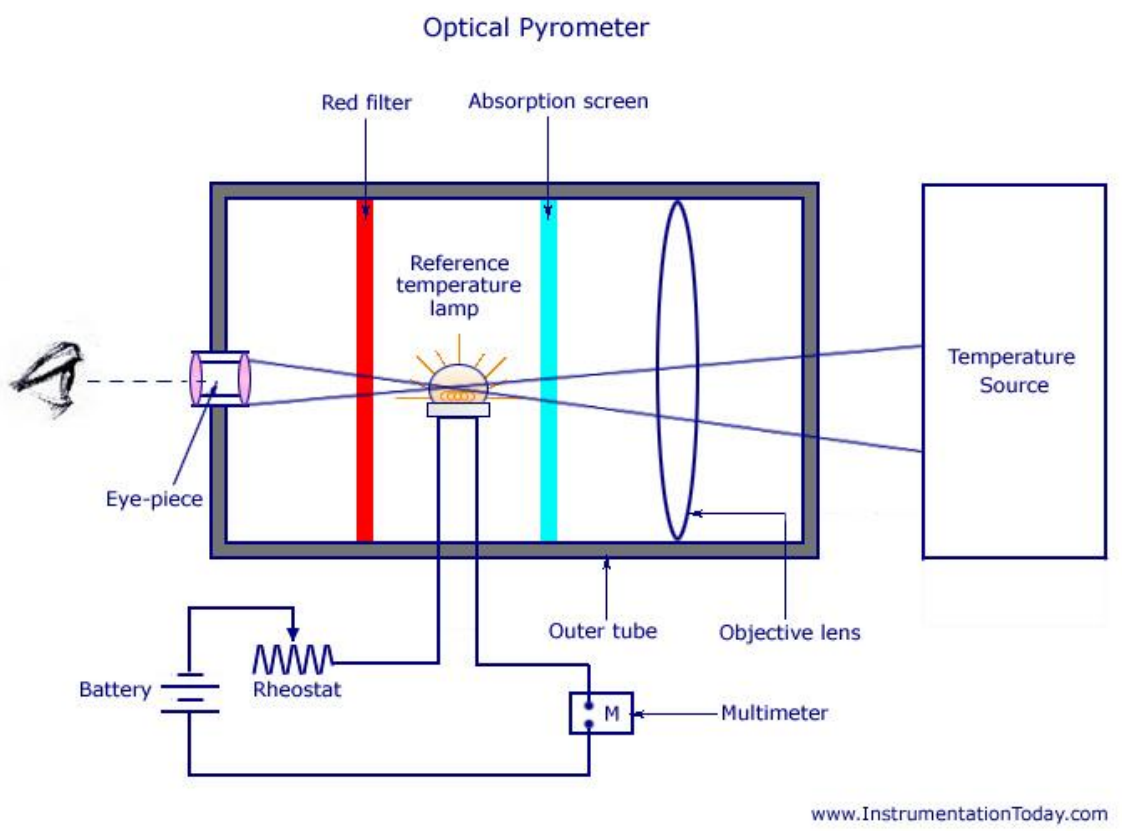

Figure 5.2 Illustration of the structure for an optical pyrometer.

Source: http://www.instrumentationtoday.com/

The process of calibration of an optical pyrometer requires establishing the brightness of the filament with different temperature. Each temperature should correspond to a brightness of the filament. When measuring the temperature of an object, the brightness of the filament needs to be checked, adjusting the rheostat until the filament disappears. When the filament disappears, which means the filament is at the same temperature as the measuring object, the temperature meter is checked and the temperature is obtained.

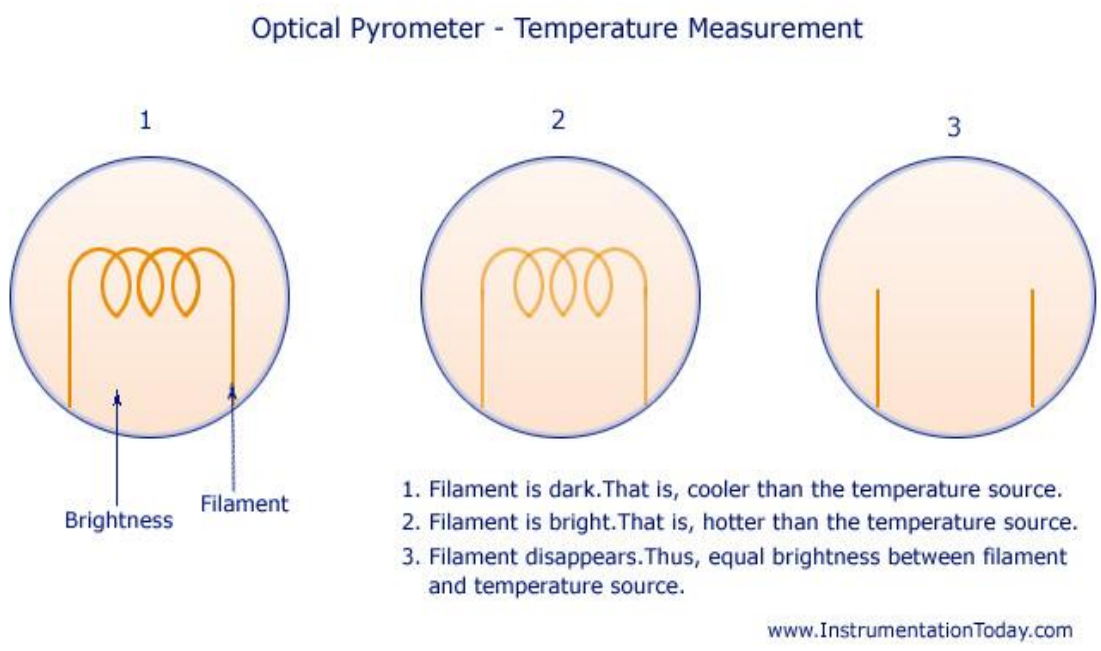

Figure 5.3 Guidelines for an optical pyrometer
http://www.instrumentationtoday.com/

5.2.1.2 Radiation Pyrometer. A radiation pyrometer reads the object's surface temperature by measuring the emission of its heat radiation. The optical system collects the infrared energy from the object's surface and sends it to the detector. The detector converts the energy into an electrical signal for the correct temperature display through the Stefan–Boltzmann law.

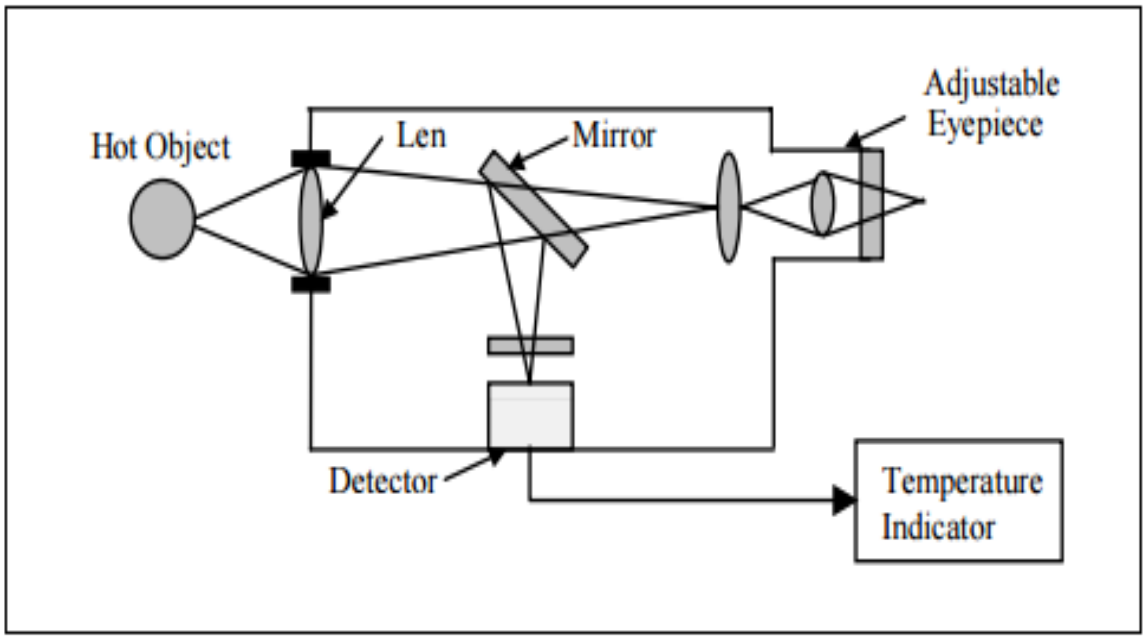

Figure 5.4 Structure of a radiation pyrometer.
Source: [21]

In semiconductor manufacturing processes, the common way of using a pyrometer, is to collect the radiation from the wafer using a quartz or sapphire rod. This type of interface has been used with PVD, HDP-CVD, RTP, Etch and RTCVD equipment offered by several major machine vendors[22].

The advantages of radiation pyrometers are as follows: (a) A radiation pyrometer can be used to measure an object at a very high temperature. For example, monitoring the temperature of molten glass and molten metal during fusing and forming operations are applications in industry manufacturing. (b) A radiation pyrometer can measure small hot objects (about 0.06 inch in diameter)[21].

5.2.3 Infrared Camera

An infrared camera, or a thermo-graphic camera, is a device that forms an image via infrared radiation, similar to a common camera that forms an image using visible light. The wavelengths of visible light are from 400nm to 700 nm, and the wavelength of infrared is more than 14,000 nm (14 µm)[23]. According to Stefan–Boltzmann law, the infrared radiation emitted by an object increases with temperature. Infrared camera can get temperature of an object, or furthermore, the temperature distribution on the surface of an object.

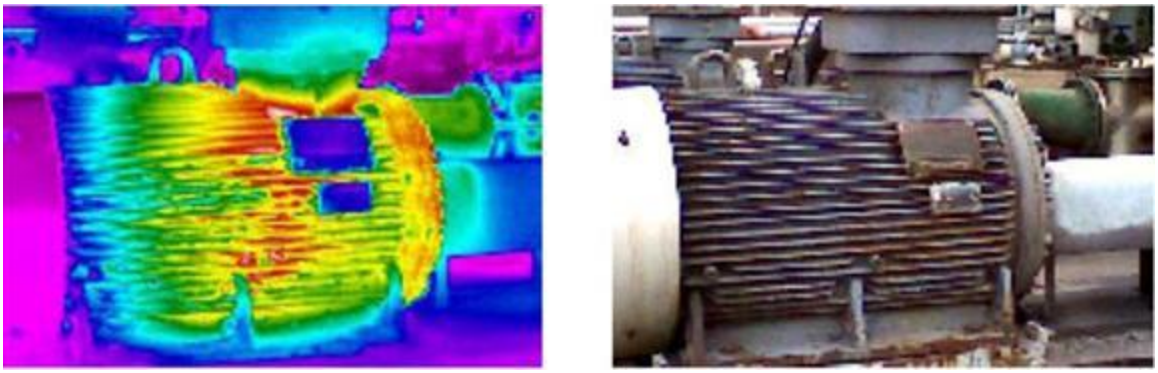

Figure 5.5 A comparison between the pictures taken by a common camera and an infrared camera

Source: http://www.infinet.com.tw/001/support_article_001.aspx?cid=C_00000007&index=41

5.2.3 Thermo-Reflectance Thermography

Thermography (TRTG) is an efficient non-contact and non-destructive optical approach for probing the steady-state and transient surface temperature. It provides accurate measurements of temperature for submicron features of microelectronic devices with excellent spatial and thermal/temperature resolutions[24].

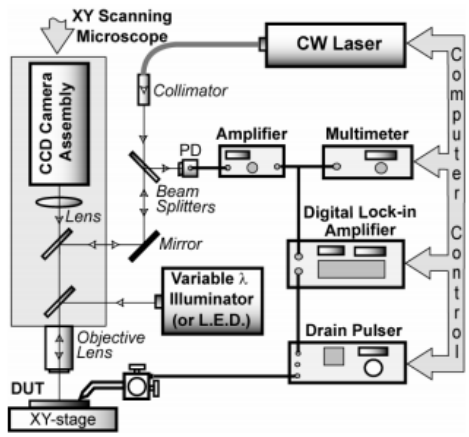

Figure 5.6 Equipment setup for thermo-reflectance method.
Source: [24]

Thermo-reflectance microscopy is based on the principle that a change in temperature of a given material produces a small change in the reflectivity of that material's surface. Thus, to measure the gradient in the temperature of a sample, ΔT, one needs to measure the relative change in the reflectivity of the sample, ΔR/R, and know the thermo-reflectance coefficient that relates them, C_{TR}. The latter is a function of the material under test, the wavelength of the probing light, and even the composition of the sample if the sample is multi-layered with transparent or semi-transparent materials present in the path of the probing light[25].

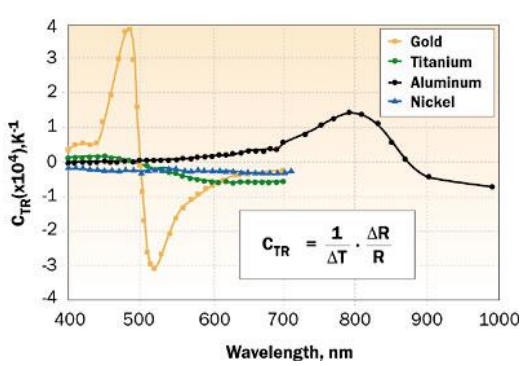

Figure 5.7 Examples of measured CTR values for selected materials.

Source:[25]

CHAPTER 6

EXPERIMENTAL DETAILS, RESULTS AND DISCUSSIONS

6.1 Experimental Details

Equipment Used in Experiments:

Digital thermometer, silicon wafer and Corning PC-35 hot plate.

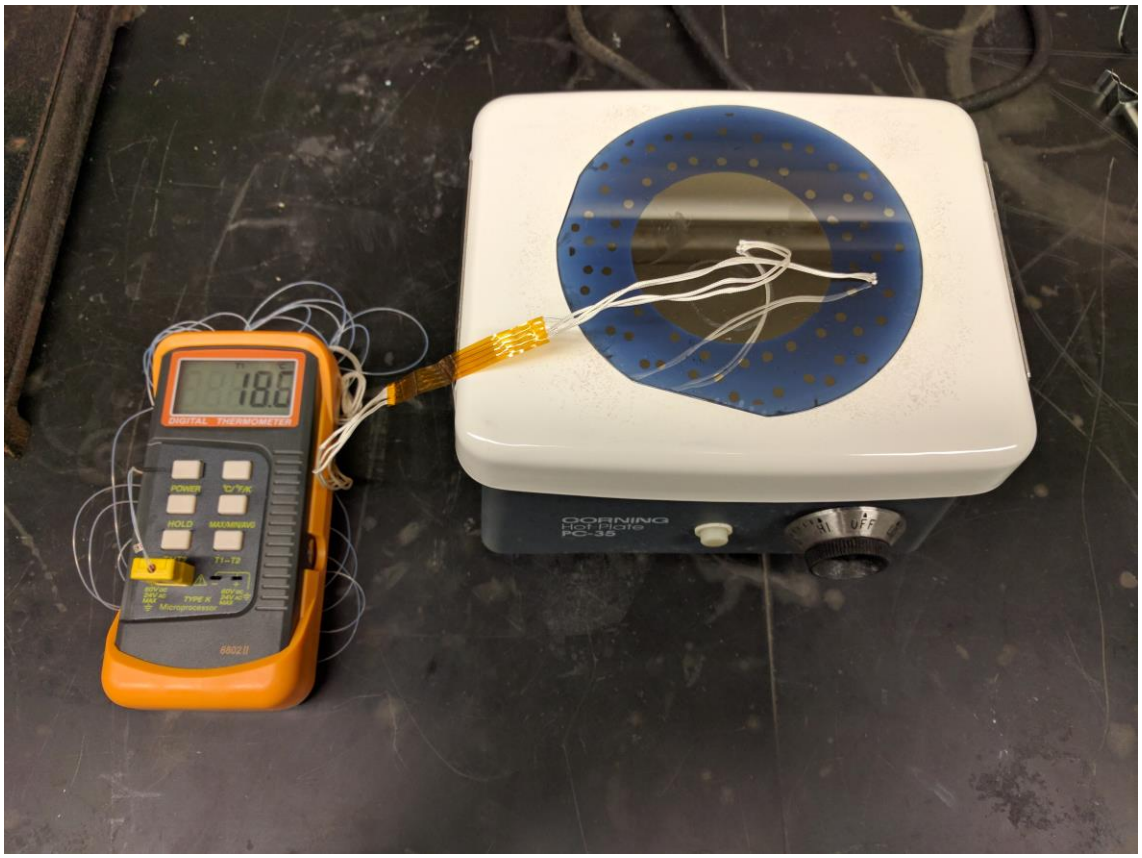

Figure 6.1 Experimental setup used in this study; the circular dots on the silicon wafer represent thermocouples embedded into Metal Oxide Semiconductor structures.

Experimental procedure:

1. Turn on the heater for 20 minutes, measuring the temperature every minute, and making sure that it is in a stable state.
2. Quickly place the wafer on the hot plate, and start the heating process.
3. Record the temperature every 5 seconds for 60 seconds.
4. Repeat the process to obtain four sets of data.

6.2 Experimental Results and Discussions

As can be seen in Figure 6.2, after 25 seconds of heating, the wafer almost reaches a saturation state at about 380K. The average temperature points, from four measurements, were taken to examine the reproducibility. The spread in the acquisition of the data in the first ten seconds is due to errors in data acquisition.

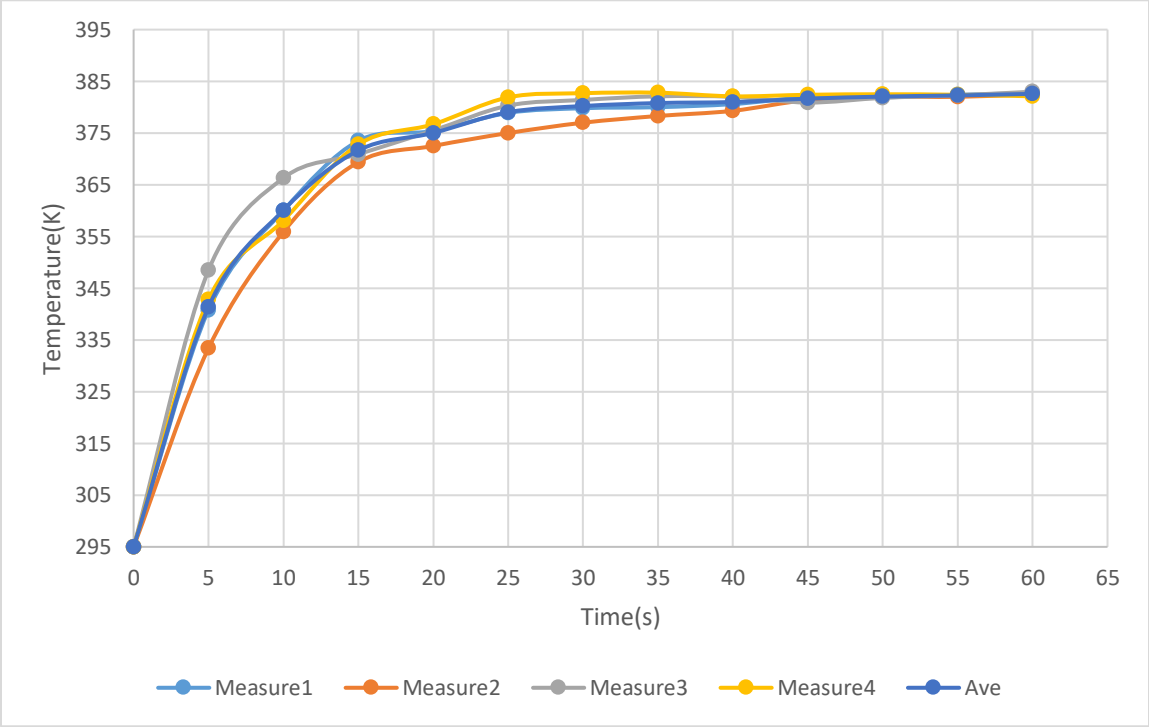

Figure 6.2 Experimental results of temperature versus time.

Table 6.1 Experimental Results

Time(s)	Measure1(K)	Measure2(K)	Measure3(K)	Measure4(K)	Ave(K)
0	295.0	295.0	295.0	295.0	295.000
5	340.8	333.4	348.5	342.8	341.375
10	360.0	355.9	366.3	358.1	360.075
15	373.5	369.4	370.9	372.8	371.650
20	375.4	372.5	375.5	376.7	375.025
25	378.9	375.0	380.3	381.9	379.025
30	379.8	377.0	381.4	382.7	380.225
35	380.0	378.3	382.1	382.8	380.800
40	380.6	379.3	382.0	382.1	381.000
45	381.9	381.4	380.9	382.4	381.650
50	381.9	382.0	381.8	382.5	382.050
55	382.4	382.0	382.3	382.4	382.275
60	382.7	382.5	383.0	382.1	382.575

.

CHAPTER 7

APPORACHES TO MODELING HEAT TRANSFER

This chapter introduces the modeling process in ANSYS CFX. The process includes: (1) Geometry, (2) Meshing, and (3) Input initial and boundary conditions, simulation and analyses of results obtained.

The first step is geometry. In order to simulate the experiment, a temperature distribution image was acquired from an infrared camera to help to create the model. The image shows that the area of highest temperature is a circle with a diameter of 8.5 cm in the center (Figure 7.1). Since the detailed emissivity of the material is not given, the infrared camera is only used to obtain the temperature distribution. Accurate temperature was measured by a thermometer, which is 393K. Based on the infrared image, a model was built (Figure 7.2).

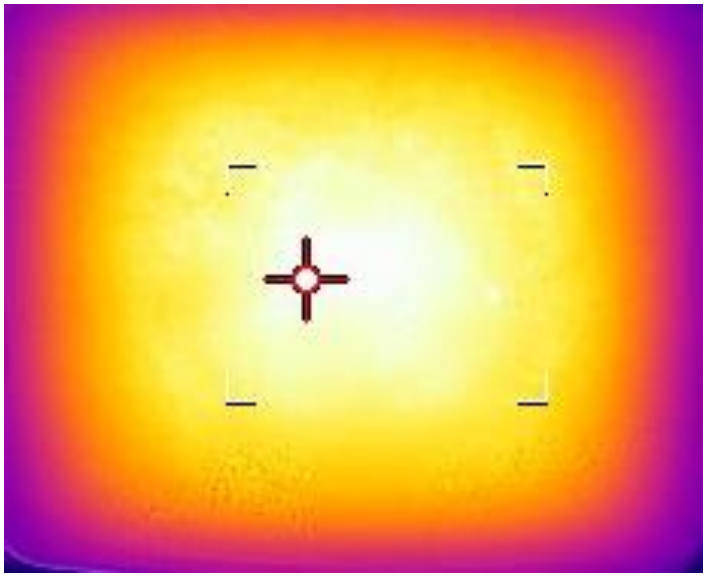

Figure 7.1 Infrared image of the hot plate.

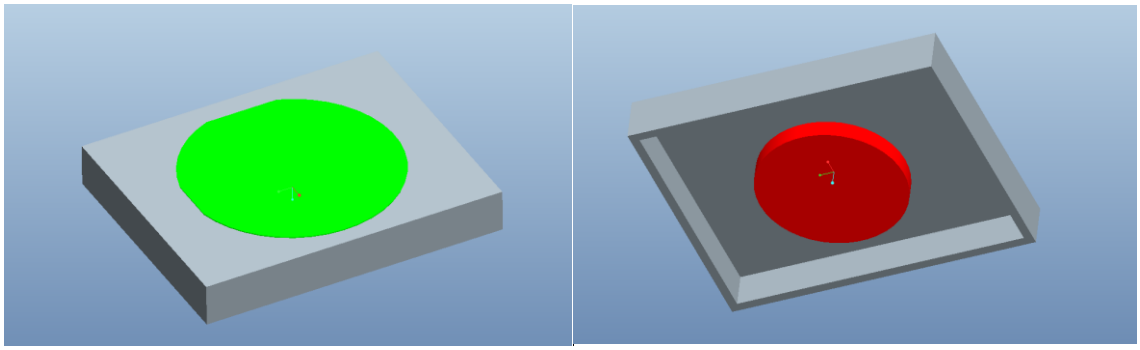

Figure 7.2 Proposed geometry based on infrared image for modeling purposes

The second step is meshing. The heat equations for heat transfer in the real world are not usually able to lead to analytical solutions. Therefore, in order to analyze heat flow, objects are split into smaller subdomains. The subdomains are called elements, and the collection of all elements is called a mesh. The heat equations are discretized and solved inside each of these elements. The more the elements are spilt, the more precise solutions are calculated. However, calculation time depends on the value of total elements. It is important to find the balance between the reliable simulation results and time budget.

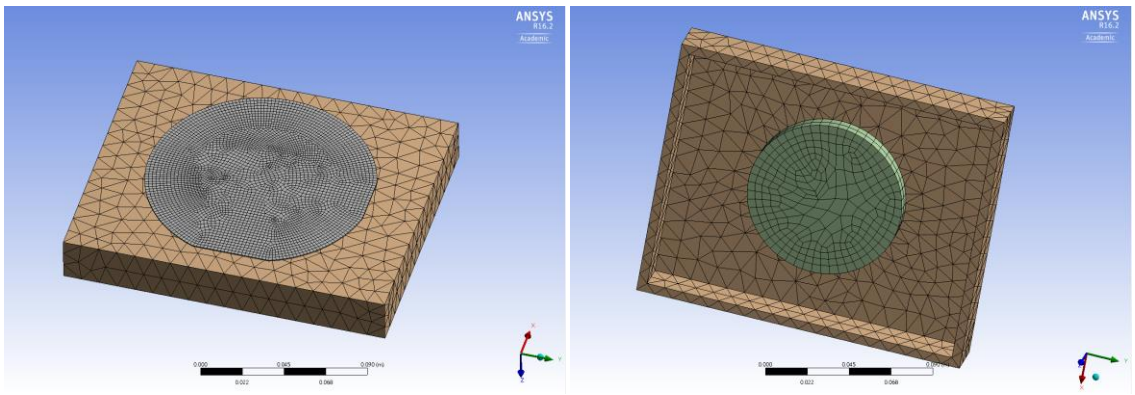

Figure 7.3 ANSYS based meshing for modeling purposes.

The third step is to input initial and boundary conditions to obtain results. The properties of silicon were introduced in Chapter 4. The initial temperature was measured from the experiment. After inputting all the properties and conditions, the program begins to simulate the results. In simulations, the Time Step size is another important parameter.

It must be small enough to resolve time-dependent features. If the value of the Time Step is too large, the solution curve will not fit to the true solution because the true solution has not been resolved. The smaller the time step, the solution is closer to the true solution. However, it takes more time to obtain the simulation results.

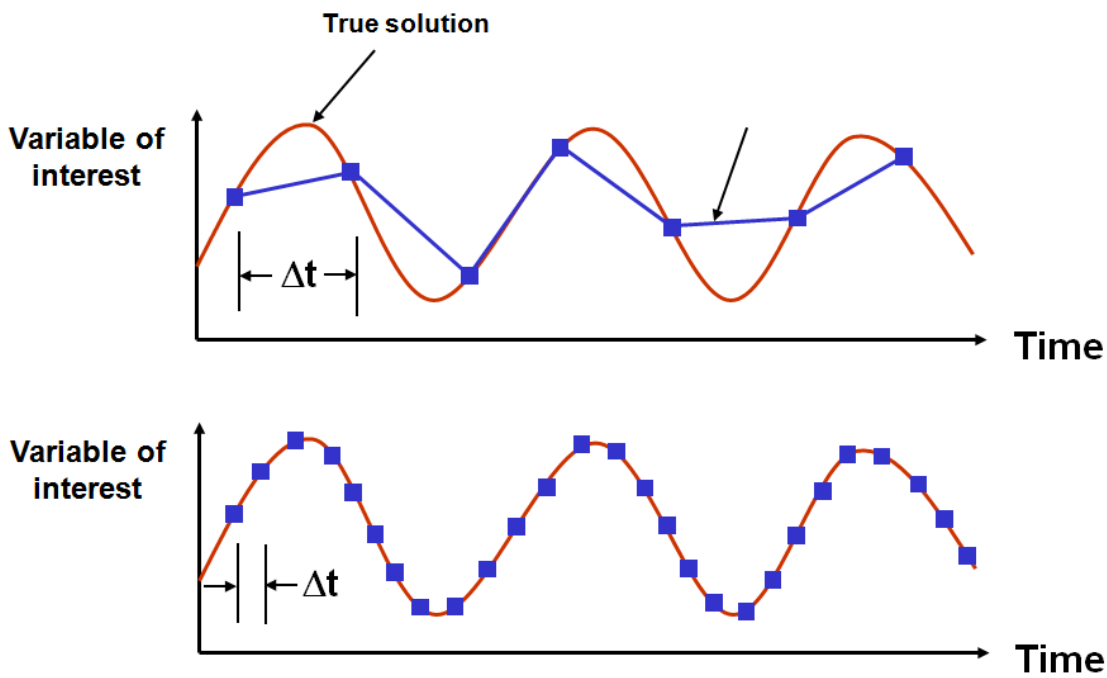

Figure 7.4 Influence of time scale on solution.

Source: ANSYS Training Manual

CHAPTER 8

RESULTS AND DISCUSSION

8.1 Simulation Approach

8.1.1 Comparison Between Different Meshing Elements

The number of meshing elements plays a significant role in a model. The more elements the model has, the more accurate the result would be calculated. However, a model with huge amount of elements takes a long time to complete the simulation. Moreover, the computer cannot afford the load for calculation. Finding a balance between accuracy and efficiency is very important. The comparison between two different meshing elements, 6940 and 24044, is shown below in Figure 8.1,

Figure 8.2 and Figure 8.3 present the temperature distribution of the silicon wafer for different meshing elements. Figure 8.4, and Table 8.1 show the data at the monitoring point, which is at the center of the wafer surface. The two factors achieve almost the same result since the geometry for the model is simple. Therefore, the smaller value of meshing number was chosen for the model since it saves computation time.

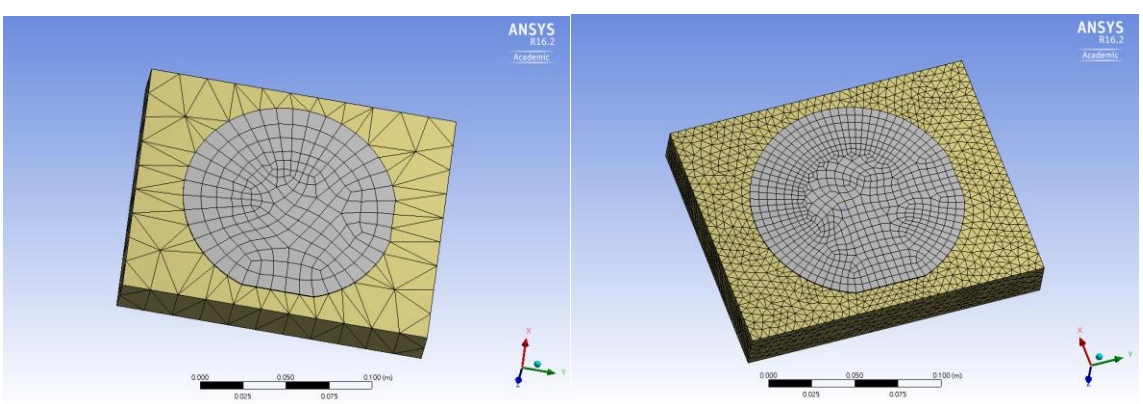

Figure 8.1 Illustration of 6940 meshing elements and 24044 meshing elements.

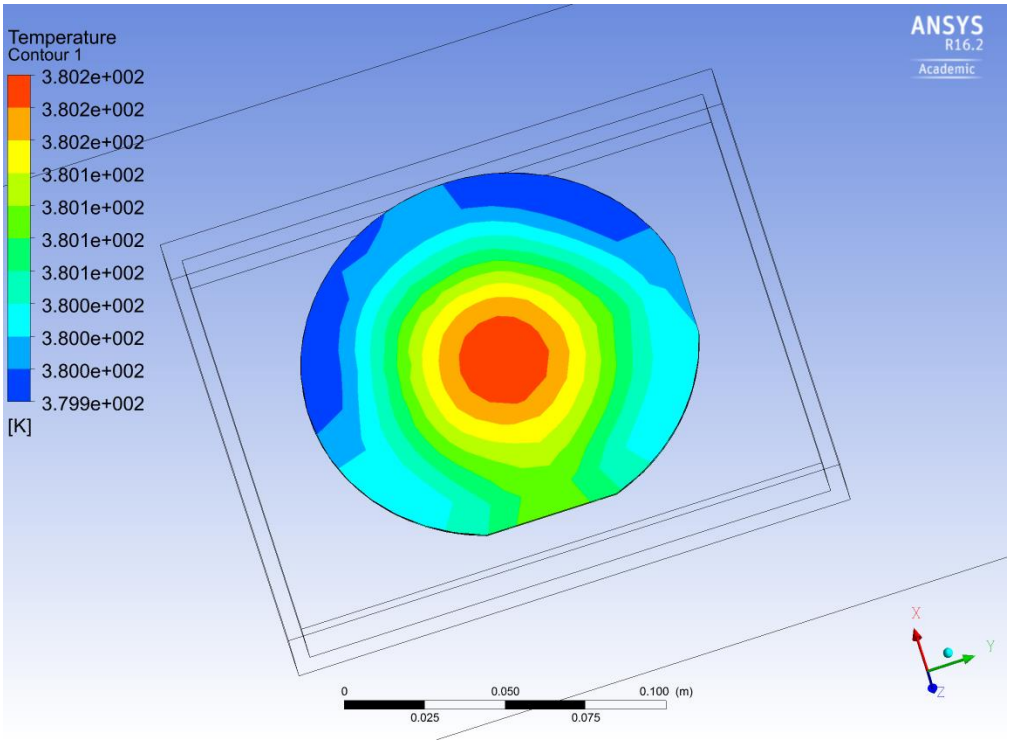

Figure 8.2 Temperature distribution of silicon wafer after heating for 60s, 6940 elements.

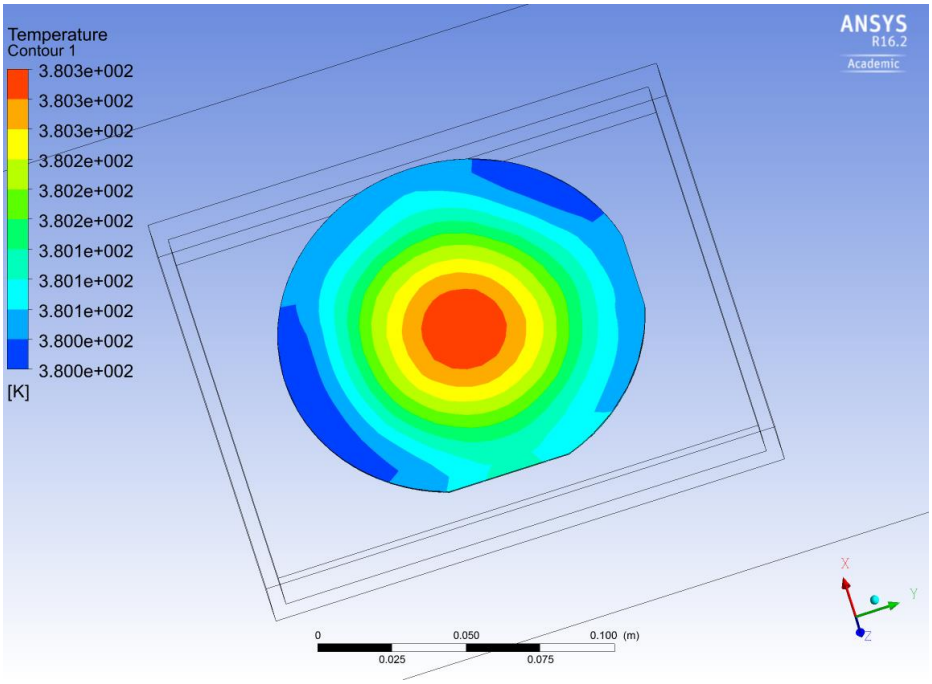

Figure 8.3 Temperature distribution of silicon wafer after heating for 60s, 24044 elements

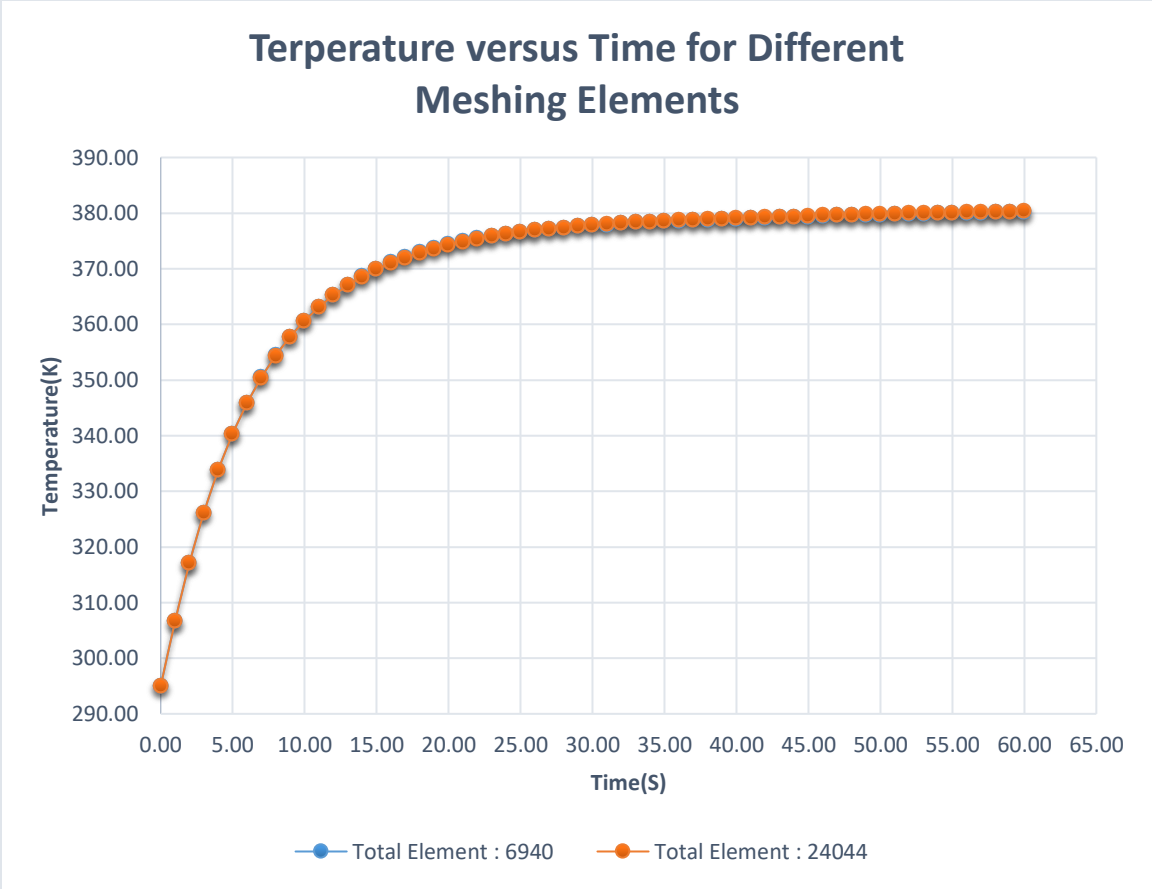

Figure 8.4 Simulated heating curve for a silicon wafer for different meshing.

Table 8.1 Simulated Temperature versus Time for 6940 and 24044 Elements

Time(s)	Total Elements : 6940	Total Elements : 24044	Time(s)	Total Elements : 6940	Total Elements : 24044	Time(s)	Total Elements : 6940	Total Elements : 24044
0	295.00	295.00	21	374.95	41.00	41	379.12	379.20
1	306.64	306.65	22	375.44	42.00	42	379.20	379.28
2	317.10	317.11	23	375.88	43.00	43	379.27	379.36
3	326.13	326.13	24	376.26	44.00	44	379.34	379.43
4	333.82	333.81	25	376.60	45.00	45	379.41	379.51
5	340.33	340.31	26	376.90	46.00	46	379.47	379.57
6	345.84	345.81	27	377.17	47.00	47	379.54	379.64
7	350.51	350.46	28	377.41	48.00	48	379.60	379.70
8	354.49	354.41	29	377.62	49.00	49	379.65	379.76
9	357.86	357.78	30	377.81	50.00	50	379.71	379.82
10	360.74	360.64	31	377.99	51.00	51	379.77	379.88
11	363.20	363.09	32	378.15	52.00	52	379.82	379.94
12	365.30	365.19	33	378.29	53.00	53	379.88	379.99
13	367.10	366.99	34	378.42	54.00	54	379.93	380.04
14	368.65	368.53	35	378.55	55.00	55	379.98	380.09
15	369.98	369.86	36	378.66	56.00	56	380.04	380.14
16	371.13	371.01	37	378.76	57.00	57	380.09	380.19
17	372.12	372.01	38	378.86	58.00	58	380.14	380.24
18	372.98	372.88	39	378.95	59.00	59	380.19	380.29
19	373.73	373.64	40	379.04	60.00	60	380.23	380.34
20	374.38	374.30						

8.1.2 Comparison Between Different Thermal Contact Resistance

In stable state temperature distribution, thermal contact resistance only motivates the final temperature. Figures 8.5 and 8.6 show the temperature distribution in stable state at different. thermal contact resistances, 0.0002 ($m^2 \cdot K \cdot W^{-1}$) and 0.009 ($m^2 \cdot K \cdot W^{-1}$).

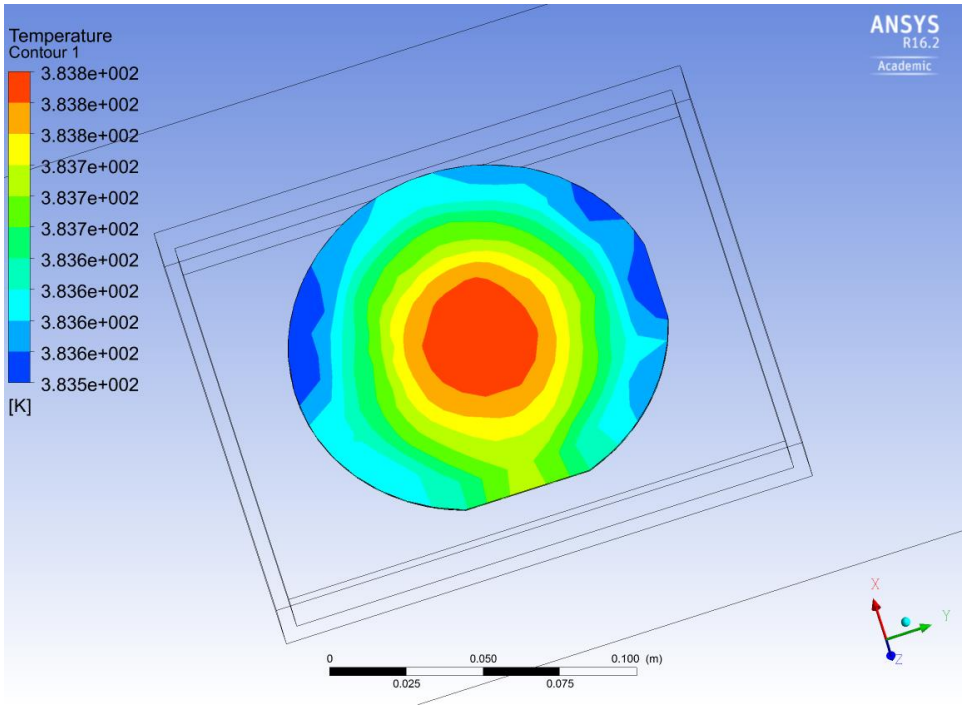

Figure 8.5 Temperature distribution of silicon wafer after heating for 60s, TCR= 0.0002($m^2 \cdot K \cdot W^{-1}$), Diameter = 5inch, Thickness = 625µm

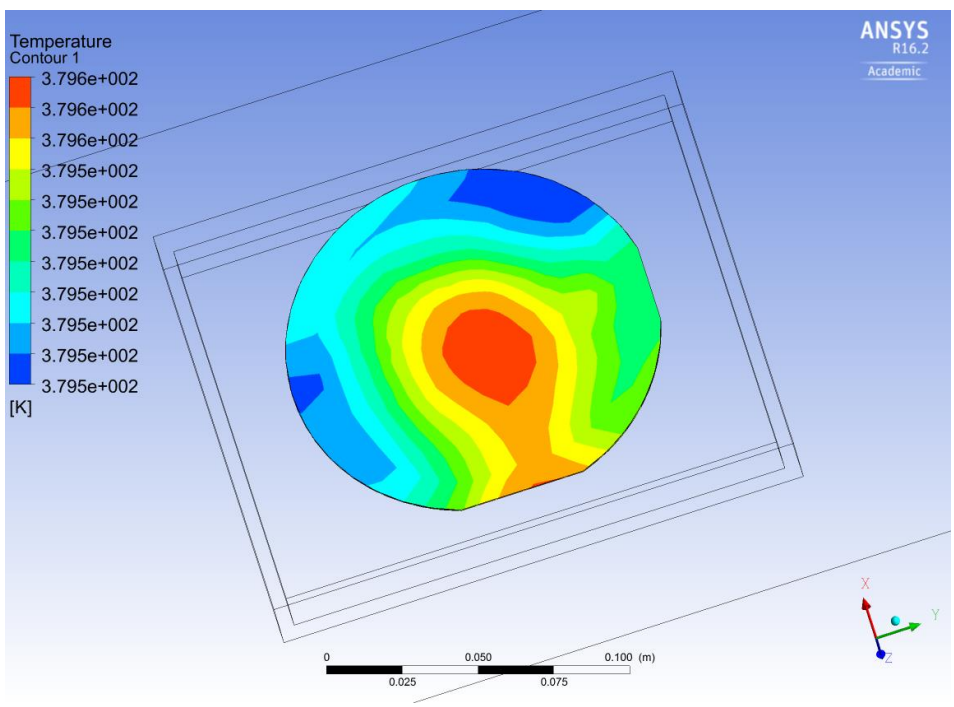

Figure 8.6 Temperature distribution of silicon wafer after heating for 60s, TCR= 0.009 ($m^2 \cdot K \cdot W^{-1}$), Diameter = 5inch, Thickness = 625µm

However, the thermal contact resistance was found to influence the shape of the curve, which means that the thermal contact resistance is a significant factor for heating process.

At TCR = 0.0002 ($m^2 \cdot K \cdot W^{-1}$), the temperature increases rapidly to the maximum point, and gently decreases to the stable temperature. This curve does not fit the experimental data. In order to find the best suitable TCR for the model, several values were input to find the best match for the experimental data (Figure 8.1 and Table 8.1). TCR = 0.006($m^2 \cdot K \cdot W^{-1}$) was chosen to be the best value. Although the stable temperature for this setup has a 3-degree error, which is less than 1%, the simulation results from 0 to 20 second matches the true solution (Figure 8.2 and Table 8.2).

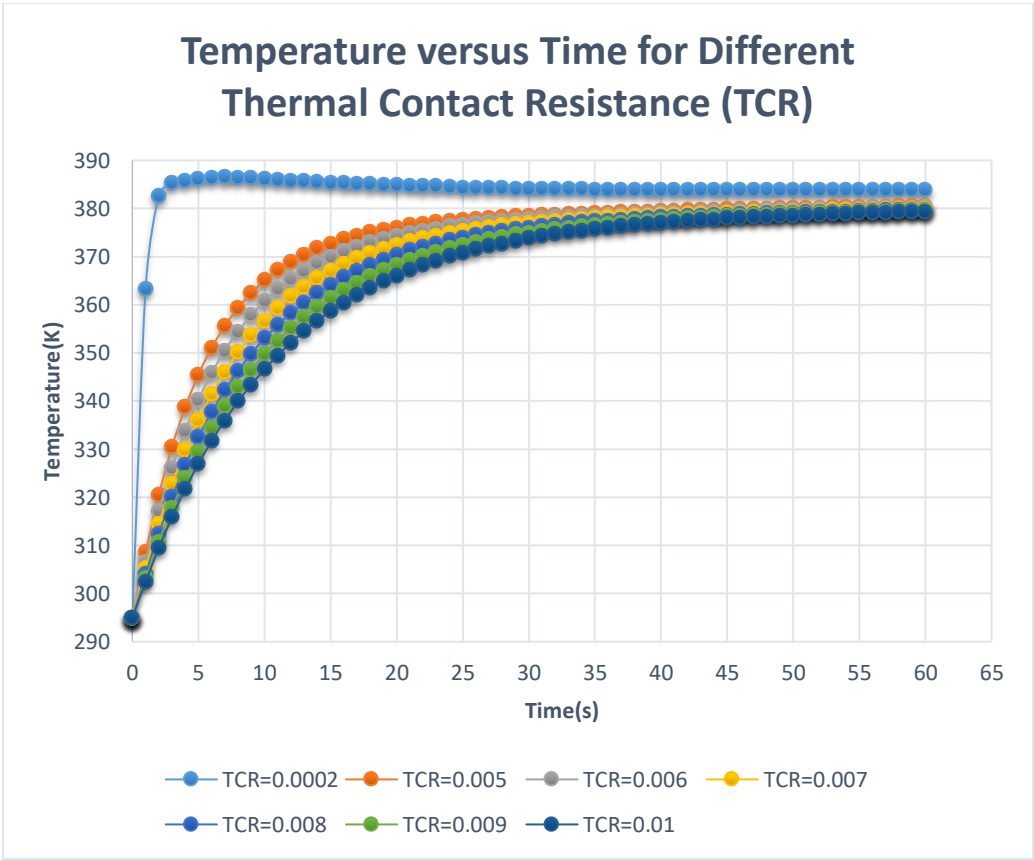

Figure 8.7 Simulation heating curves for a silicon wafer for different thermal contact resistance ($m^2 \cdot K \cdot W^{-1}$).

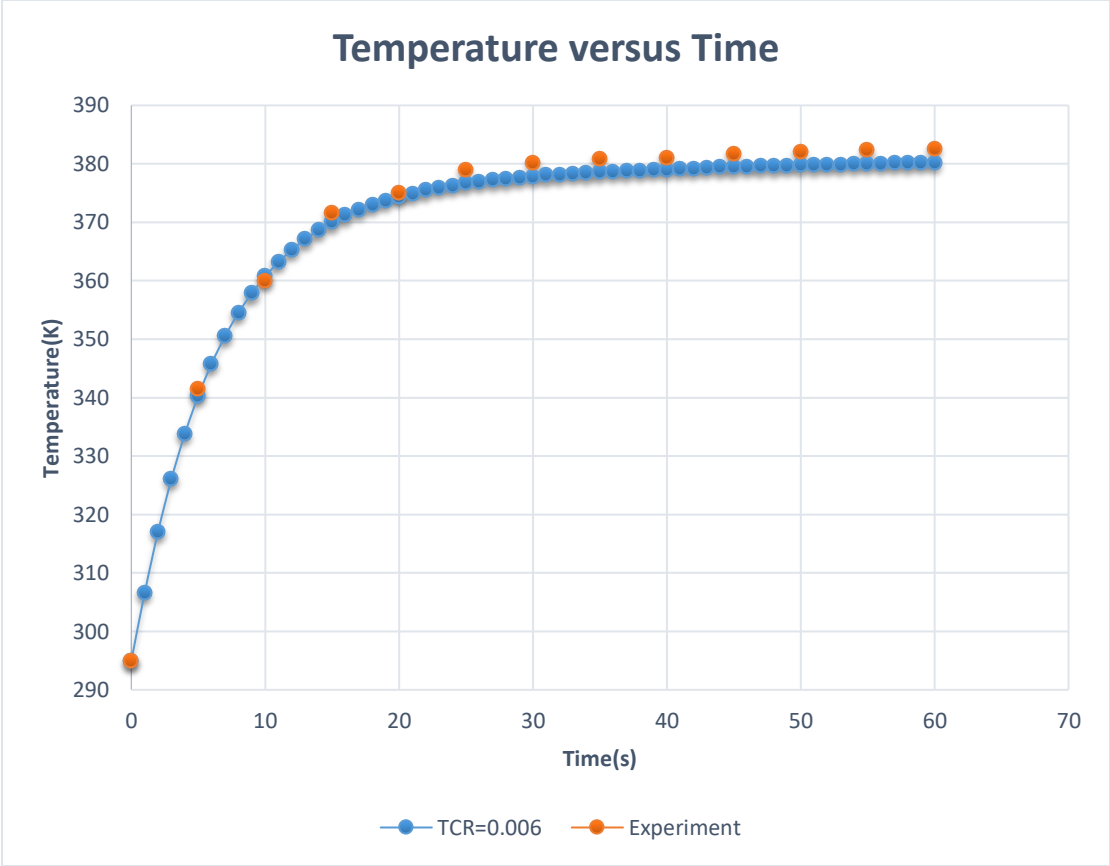

Figure 8.8 Simulated heating curve (TCR = 0.006 ($m^2 \cdot K \cdot W^{-1}$)) and experimental heating curve.

Table 8.2 Simulated Temperature (K) for Different Thermal Contact Resistance($m^2 \cdot K \cdot W^{-1}$)

Time(s)	TCR=0.0002	TCR=0.005	TCR=0.006	TCR=0.007	TCR=0.008	TCR=0.009	TCR=0.01
0	295.00	295.00	295.00	295.00	295.00	295.00	295.00
1	363.32	308.55	306.64	305.21	304.10	303.21	302.48
2	382.69	320.47	317.10	314.52	312.49	310.84	309.48
3	385.31	330.48	326.13	322.72	319.99	317.76	315.88
4	385.69	338.74	333.82	329.87	326.64	323.96	321.69
5	386.11	345.52	340.33	336.06	332.50	329.51	326.94
6	386.39	351.07	345.84	341.43	337.67	334.47	331.69
7	386.47	355.63	350.51	346.09	342.24	338.91	335.99
8	386.42	359.39	354.49	350.13	346.27	342.89	339.88
9	386.29	362.48	357.86	353.65	349.84	346.46	343.41
10	386.14	365.05	360.74	356.71	353.00	349.65	346.61
11	385.99	367.18	363.20	359.39	355.80	352.53	349.51
12	385.83	368.96	365.30	361.72	358.29	355.10	352.14
13	385.68	370.44	367.10	363.75	360.49	357.42	354.52
14	385.54	371.69	368.65	365.53	362.45	359.50	356.69
15	385.40	372.74	369.98	367.09	364.19	361.37	358.66
16	385.27	373.63	371.13	368.47	365.74	363.05	360.44
17	385.15	374.38	372.12	369.67	367.12	364.57	362.07
18	385.03	375.03	372.98	370.73	368.35	365.94	363.56
19	384.92	375.58	373.73	371.66	369.45	367.18	364.90
20	384.82	376.05	374.38	372.48	370.43	368.29	366.13
21	384.73	376.46	374.95	373.21	371.30	369.29	367.25
22	384.64	376.82	375.44	373.86	372.09	370.20	368.27
23	384.56	377.13	375.88	374.43	372.79	371.03	369.20
24	384.48	377.40	376.26	374.94	373.42	371.77	370.05
25	384.41	377.64	376.60	375.39	373.98	372.44	370.82
26	384.35	377.85	376.90	375.79	374.49	373.05	371.53
27	384.29	378.04	377.17	376.15	374.95	373.61	372.18
28	384.23	378.21	377.41	376.47	375.36	374.12	372.77
29	384.18	378.37	377.62	376.76	375.74	374.58	373.31
30	384.13	378.51	377.81	377.02	376.08	375.00	373.81

Table 8.3 Simulated Temperature(K) for Different Thermal Contact Resistance ($m^2 \cdot K \cdot W^{-1}$) (Continued)

Time(s)	TCR=0.0002	TCR=0.005	TCR=0.006	TCR=0.007	TCR=0.008	TCR=0.009	TCR=0.01
31	384.09	378.63	377.99	377.25	376.38	375.38	374.27
32	384.05	378.75	378.15	377.46	376.66	375.73	374.69
33	384.02	378.86	378.29	377.66	376.91	376.04	375.08
34	383.98	378.96	378.42	377.84	377.14	376.33	375.43
35	383.95	379.05	378.55	378.00	377.35	376.60	375.75
36	383.93	379.14	378.66	378.15	377.54	376.84	376.05
37	383.90	379.23	378.76	378.29	377.72	377.07	376.33
38	383.88	379.31	378.86	378.41	377.88	377.27	376.58
39	383.86	379.39	378.95	378.53	378.04	377.47	376.82
40	383.85	379.46	379.04	378.63	378.17	377.64	377.04
41	383.83	379.53	379.12	378.73	378.30	377.81	377.24
42	383.82	379.59	379.20	378.82	378.42	377.96	377.43
43	383.81	379.66	379.27	378.91	378.53	378.10	377.60
44	383.80	379.72	379.34	378.99	378.64	378.24	377.77
45	383.79	379.78	379.41	379.07	378.74	378.36	377.92
46	383.79	379.84	379.47	379.15	378.83	378.47	378.06
47	383.78	379.90	379.54	379.23	378.92	378.58	378.20
48	383.78	379.96	379.60	379.30	379.00	378.68	378.32
49	383.78	380.02	379.65	379.36	379.07	378.78	378.44
50	383.78	380.08	379.71	379.42	379.15	378.87	378.55
51	383.78	380.13	379.77	379.48	379.22	378.96	378.66
52	383.78	380.18	379.82	379.54	379.29	379.04	378.75
53	383.79	380.24	379.88	379.60	379.36	379.11	378.85
54	383.79	380.29	379.93	379.65	379.42	379.19	378.94
55	383.80	380.34	379.98	379.71	379.49	379.26	379.02
56	383.81	380.38	380.04	379.76	379.55	379.33	379.10
57	383.81	380.43	380.09	379.82	379.60	379.39	379.18
58	383.82	380.47	380.14	379.87	379.66	379.45	379.25
59	383.83	380.52	380.19	379.91	379.71	379.52	379.32
60	383.84	380.57	380.23	379.96	379.77	379.57	379.38

Table 8.4 Comparison of Simulated versus Experimental Temperature(K)
(TCR = 0.006 ($m^2 \cdot K \cdot W^{-1}$))

Time(s)	Simulated	Experimental	Time(s)	Simulated	Experimental	Time(s)	Simulated	Experimental
0	295.00	295.000	21	374.95		41	379.12	
1	306.64		22	375.44		42	379.20	
2	317.10		23	375.88		43	379.27	
3	326.13		24	376.26		44	379.34	
4	333.82		25	376.60	379.025	45	379.41	381.650
5	340.33	341.375	26	376.90		46	379.47	
6	345.84		27	377.17		47	379.54	
7	350.51		28	377.41		48	379.60	
8	354.49		29	377.62		49	379.65	
9	357.86		30	377.81	380.225	50	379.71	382.050
10	360.74	360.075	31	377.99		51	379.77	
11	363.20		32	378.15		52	379.82	
12	365.30		33	378.29		53	379.88	
13	367.10		34	378.42		54	379.93	
14	368.65		35	378.55	380.800	55	379.98	382.275
15	369.98	371.65	36	378.66		56	380.04	
16	371.13		37	378.76		57	380.09	
17	372.12		38	378.86		58	380.14	
18	372.98		39	378.95		59	380.19	
19	373.73		40	379.04	381.000	60	380.23	382.575
20	374.38	375.025						

8.2 Input of Parameters

After comparing the simulated results with the experimental data, the various parameters were input to determine the temperature distribution and heating curves.

8.2.1 Comparison of Results for Different Thicknesses

The 5-inch silicon wafer, used in these experiments, is 625 µm thick. In order to observe the trend in heating time-wafer temperature versus wafer thickness, 937.5µm (1.5x wafer thickness), 1250µm (2x wafer thickness), 1562.5µm (2.5x wafer thickness) and 1875µm

(3x wafer thickness) were chosen to be input to the model. These wafers, with different thicknesses, have similar temperature distribution results, as shown in Figures 8.9 to 8.12.

The heating time required to reach the same temperature is proportional to the wafer thickness, which is in accord with expectations. This is because the heating area remains the same, thicker objects demand more energy in the heating process. Table 8.4 and Figure 8.13 show the heating time required to heat the wafer to 350 K. The simulated results are shown in Figure 8.13 and Table 8.5.

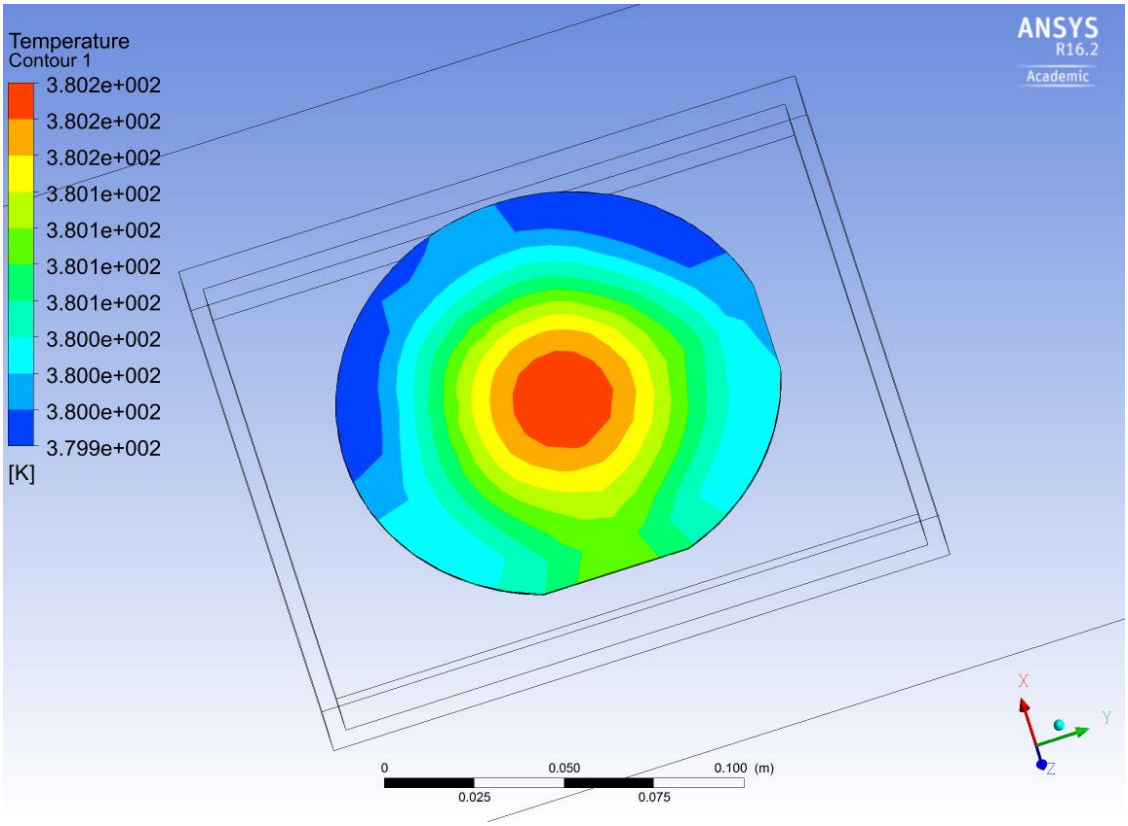

Figure 8.9 Temperature distribution of 5-inch silicon wafer after heating for 60s, thickness = 625µm.

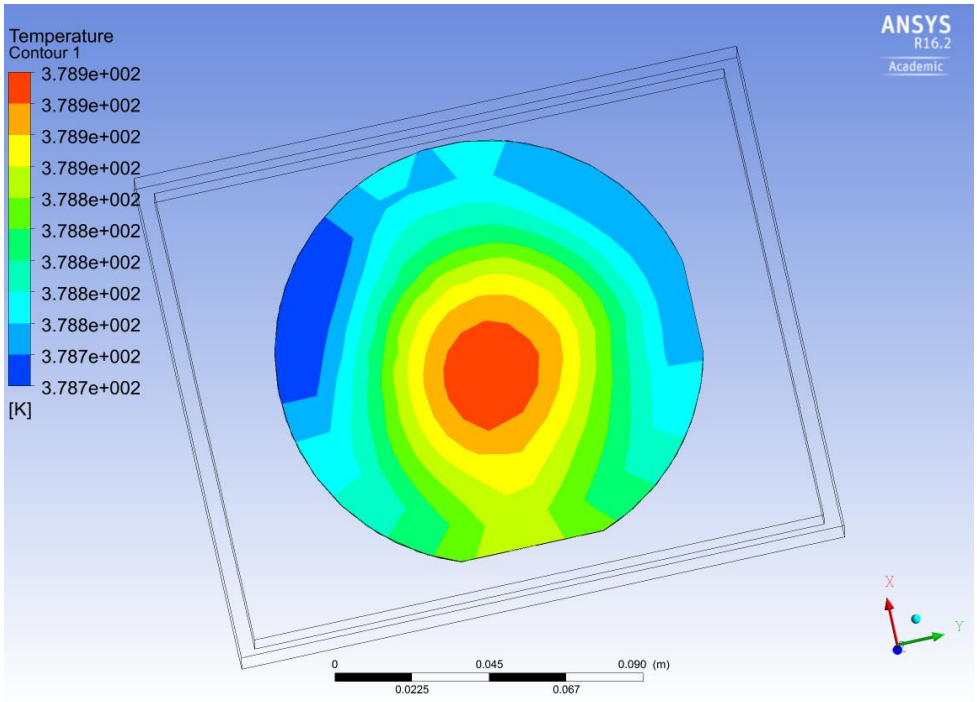

Figure 8.10 Temperature distribution of 5-inch silicon wafer after heating for 60s, thickness = 937.5μm.

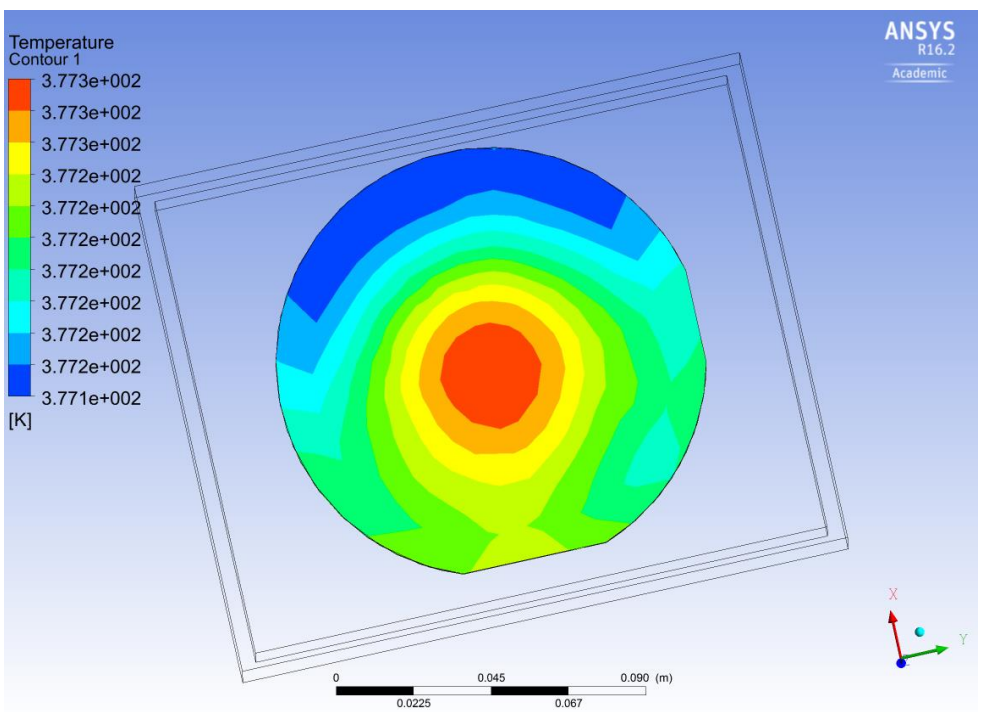

Figure 8.11 Temperature distribution of 5-inch silicon wafer after heating for 60s, thickness = 1250μm.

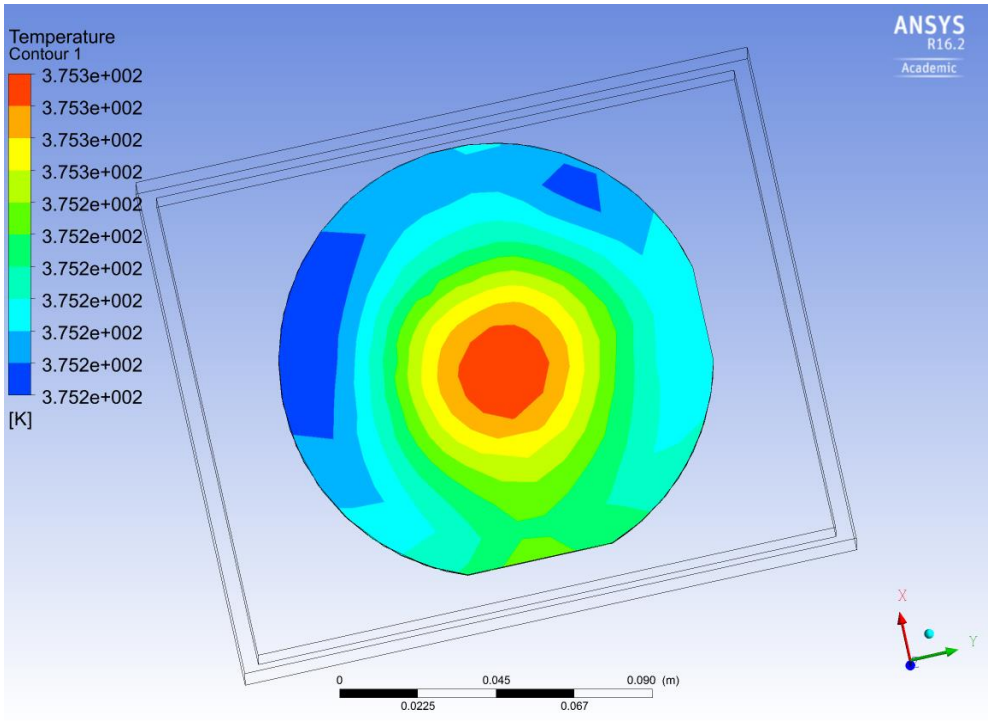

Figure 8.12 Temperature distribution of 5-inch silicon wafer after heating for 60s, thickness = 1562.5µm.

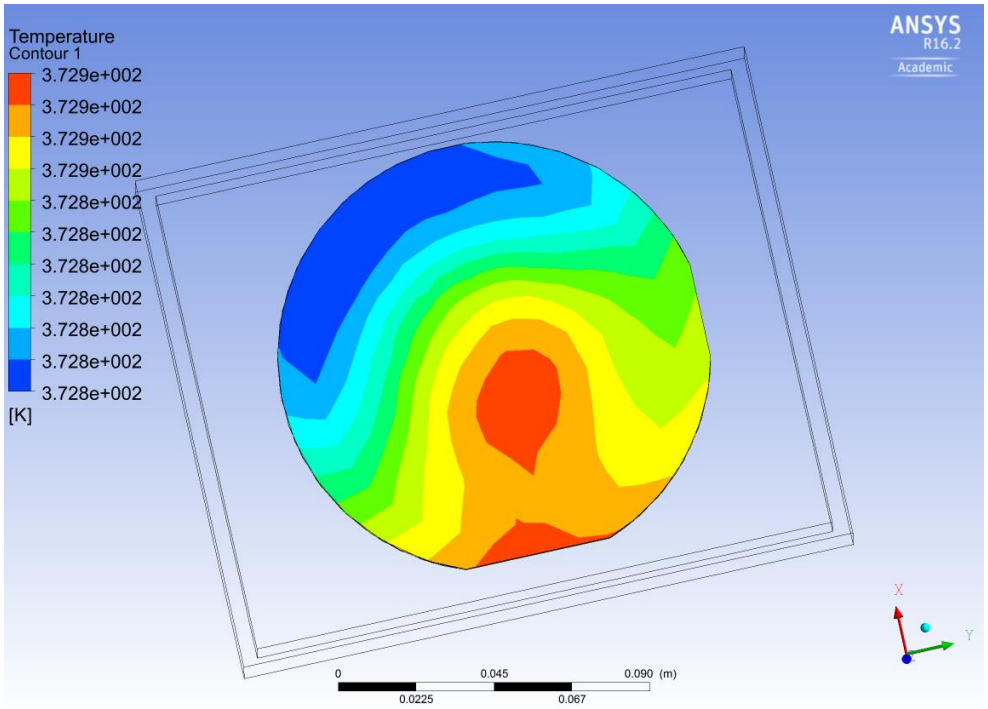

Figure 8.13 Temperature distribution of 5-inch silicon wafer after heating for 60s, thickness = 1875µm.

Table 8.5 Simulated Results of Heating Time Required to Heat the Wafer to 350 K

Thickness (µm)	625 (1x)	937.5 (1.5x)	1250 (2x)	1562.5 (2.5x)	1875 (3x)
Time (s)	7	10.5	14	18	22

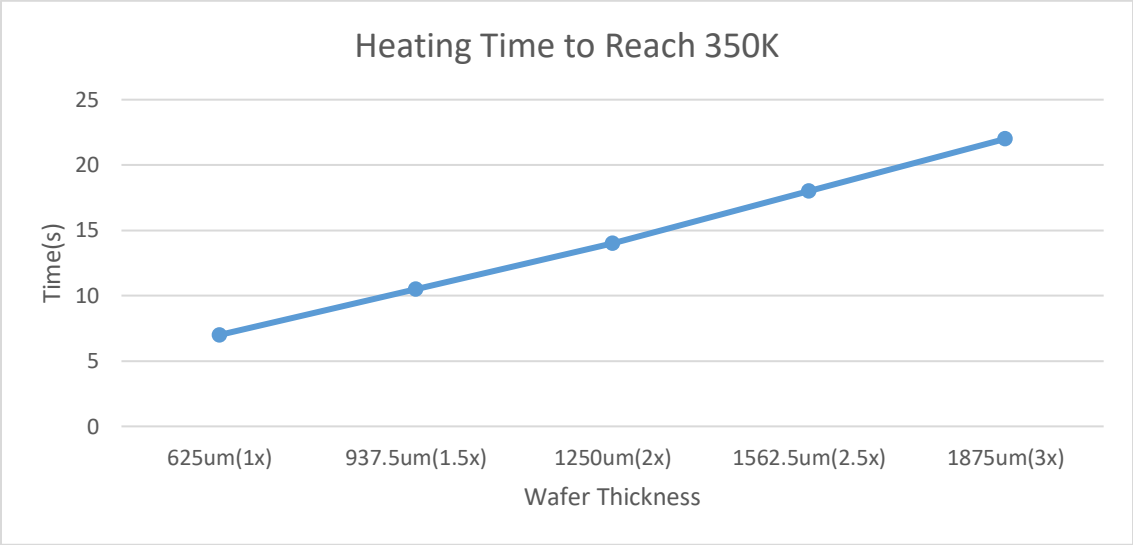

Figure 8.14 Heating time required to heat the wafer to 350K.

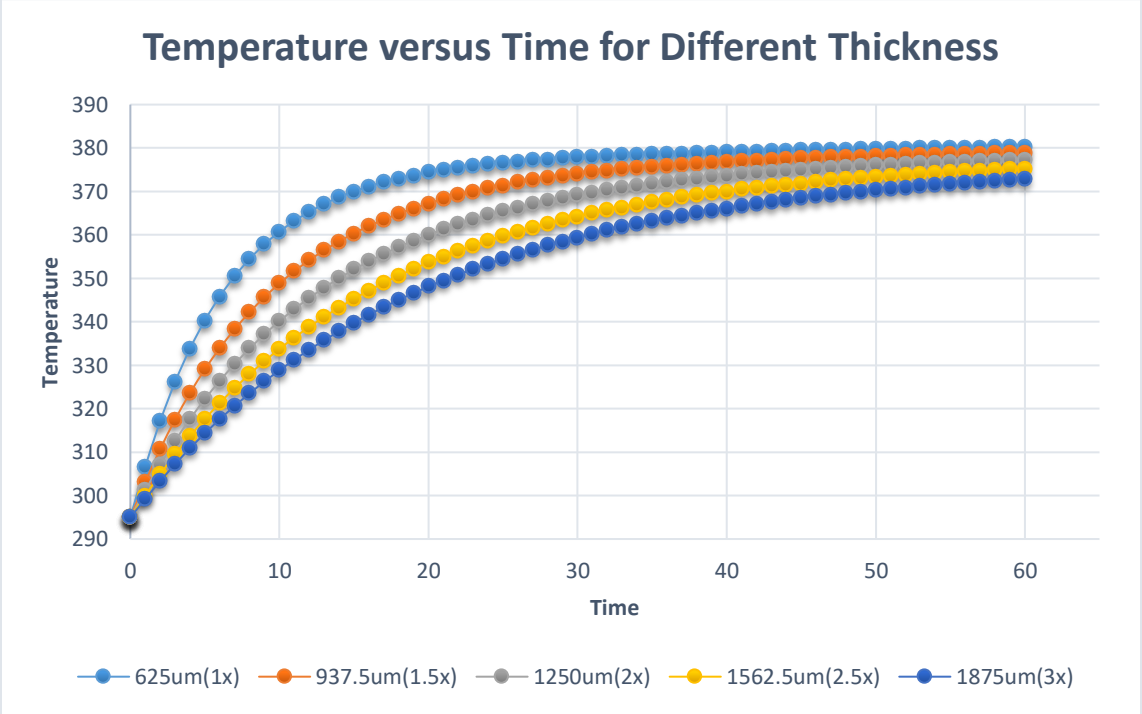

Figure 8.15 Heating curves for a 5-inch silicon wafer for different thicknesses.

Table 8.6 Temperature (K) versus Time (s) for a 5-inch Silicon Wafer for Different Thicknesses (µm)

Time (s)	625µm (1x)	937.5 µm (1.5x)	1250 µm (2x)	1562.5 µm (2.5x)	1875 µm (3x)
0	295	295	295	295	295
1	306.64	303.12	301.23	300.06	299.24
2	317.10	310.67	307.14	304.90	303.34
3	326.13	317.50	312.60	309.45	307.22
4	333.82	323.60	317.61	313.69	310.88
5	340.33	329.06	322.20	317.63	314.33
6	345.84	333.93	326.42	321.32	317.58
7	350.51	338.29	330.29	324.75	320.64
8	354.49	342.19	333.85	327.95	323.53
9	357.86	345.69	337.13	330.95	326.25
10	360.74	348.82	340.14	333.75	328.83
11	363.20	351.64	342.92	336.37	331.27
12	365.30	354.17	345.48	338.82	333.57
13	367.10	356.45	347.84	341.12	335.75
14	368.65	358.50	350.02	343.27	337.81
15	369.98	360.35	352.03	345.29	339.77
16	371.13	362.02	353.89	347.18	341.62
17	372.12	363.52	355.61	348.95	343.37
18	372.98	364.88	357.19	350.61	345.02
19	373.73	366.11	358.66	352.17	346.60
20	374.38	367.22	360.02	353.64	348.09
21	374.95	368.22	361.28	355.02	349.50
22	375.44	369.13	362.45	356.31	350.84
23	375.88	369.96	363.53	357.52	352.11
24	376.26	370.72	364.53	358.67	353.31
25	376.60	371.40	365.46	359.74	354.46
26	376.90	372.02	366.32	360.75	355.54
27	377.17	372.59	367.12	361.70	356.57
28	377.41	373.10	367.86	362.59	357.55
29	377.62	373.57	368.55	363.43	358.48
30	377.81	374.01	369.20	364.22	359.36

Table 8.7 Temperature (K) versus Time (s) for a 5-inch Silicon Wafer for Different Thicknesses (µm) (Continued)

Time (s)	625µm (1x)	937.5 µm (1.5x)	1250 µm (2x)	1562.5 µm (2.5x)	1875 µm (3x)
31	377.99	374.40	369.79	364.97	360.20
32	378.15	374.76	370.35	365.67	361.00
33	378.29	375.09	370.87	366.33	361.76
34	378.42	375.40	371.35	366.95	362.48
35	378.55	375.68	371.81	367.54	363.16
36	378.66	375.94	372.23	368.10	363.81
37	378.76	376.18	372.62	368.62	364.43
38	378.86	376.40	372.99	369.11	365.02
39	378.95	376.60	373.33	369.58	365.58
40	379.04	376.79	373.65	370.02	366.12
41	379.12	376.97	373.95	370.44	366.63
42	379.20	377.13	374.24	370.83	367.11
43	379.27	377.28	374.50	371.20	367.57
44	379.34	377.43	374.75	371.55	368.01
45	379.41	377.56	374.99	371.89	368.43
46	379.47	377.69	375.20	372.20	368.83
47	379.54	377.81	375.41	372.51	369.21
48	379.60	377.92	375.61	372.79	369.58
49	379.65	378.02	375.79	373.06	369.93
50	379.71	378.12	375.97	373.32	370.26
51	379.77	378.22	376.13	373.56	370.58
52	379.82	378.31	376.29	373.79	370.88
53	379.88	378.40	376.44	374.01	371.17
54	379.93	378.49	376.58	374.22	371.45
55	379.98	378.57	376.71	374.42	371.71
56	380.04	378.64	376.84	374.61	371.96
57	380.09	378.71	376.96	374.79	372.21
58	380.14	378.78	377.07	374.97	372.44
59	380.19	378.85	377.19	375.13	372.66
60	380.23	378.92	377.29	375.29	372.87

8.2.2 Comparison of Results for Different Diameters

Wafers of diameters of 1-inch, 2-inch and 5-inch silicon wafers were input to the model. According to Fourier's law, the three wafers should have the same heating trend since the heat flux through the contacting surfaces are the same. However, there are slight differences due to the different thermal contact resistance. Simulated results match the theory. Figures 8.14 to 8.16 demonstrate the temperature distribution. Figure 8.17 and Table 8.6 show the simulation results.

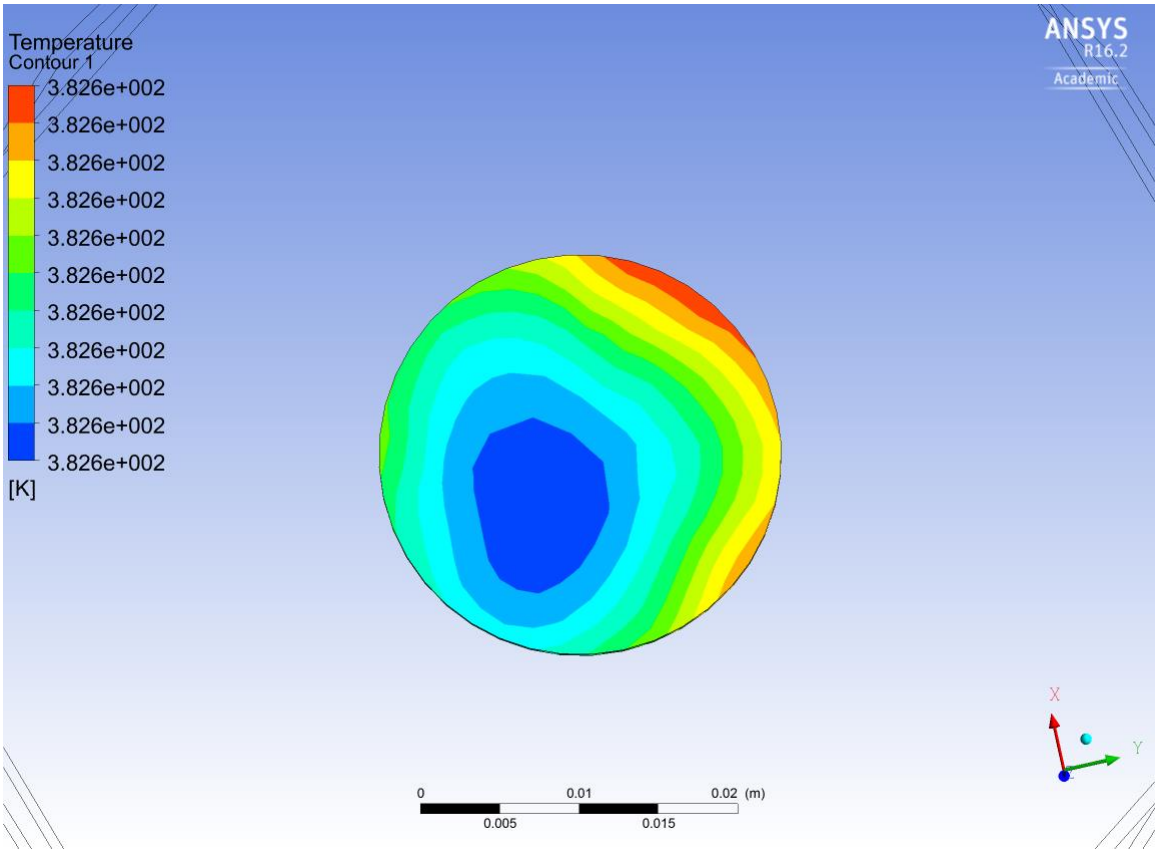

Figure 8.16 Temperature distribution of silicon wafer after heating for 60s, Thickness = 625μm, Diameter = 1inch.

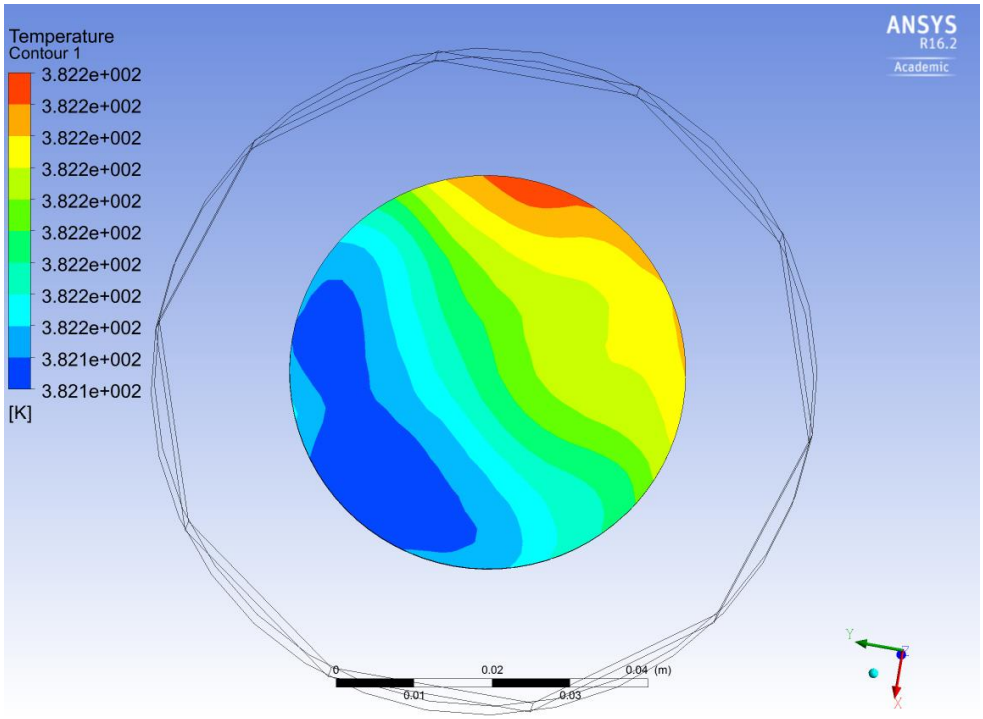

Figure 8.17 Temperature distribution of silicon wafer after heating for 60s, Thickness = 625µm, Diameter = 2inch.

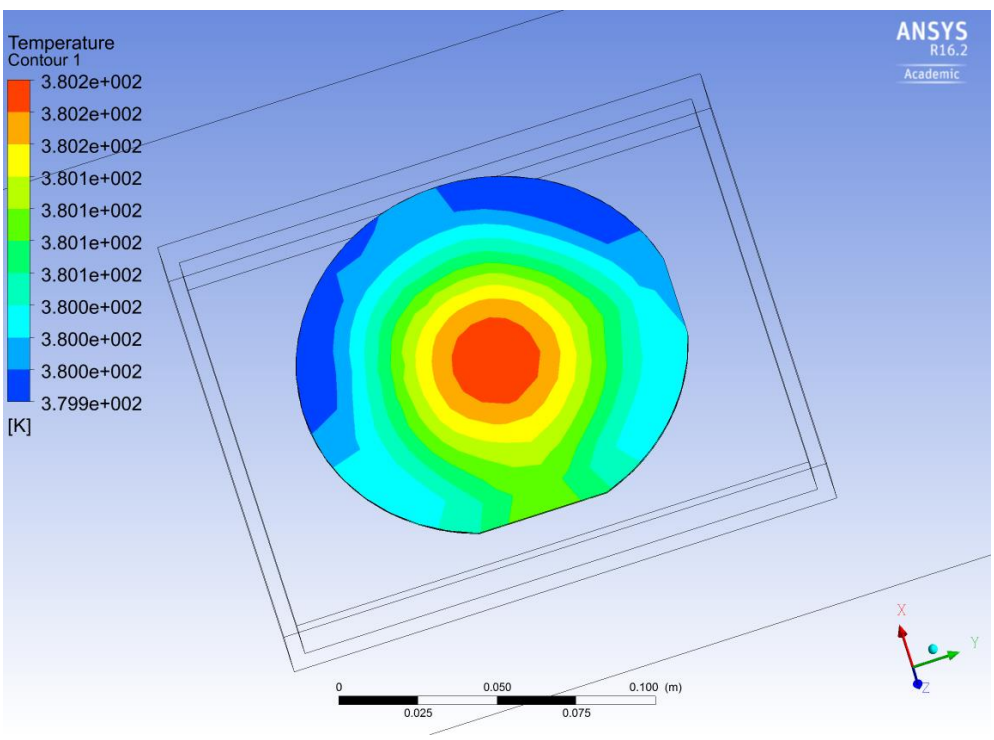

Figure 8.18 Temperature distribution of silicon wafer after heating for 60s, Thickness = 625µm, Diameter = 5inch.

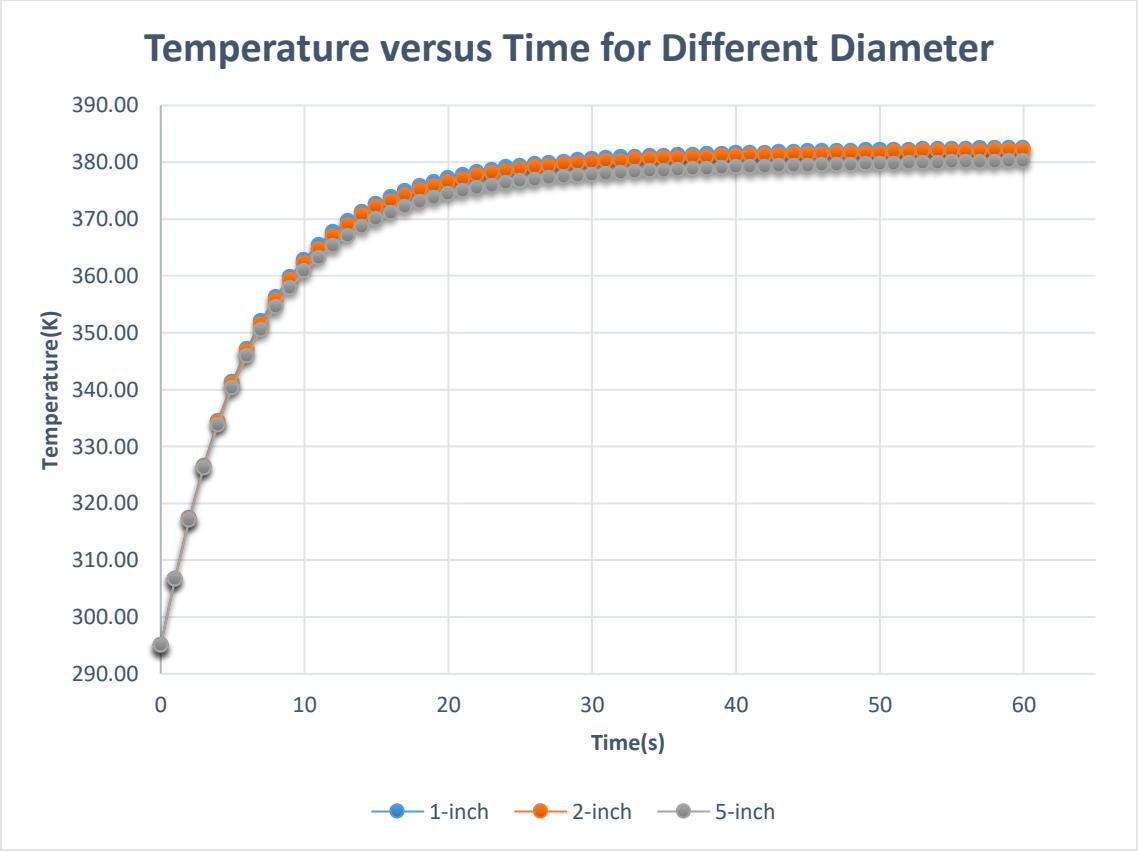

Figure 8.19 Simulated heating curves of silicon wafer for different diameters.

Table 8.8 Simulated Temperature (K) versus Time (s) for a Silicon Wafer for Different Diameters

Time (s)	1-inch	2-inch	5-inch	Time (s)	1-inch	2-inch	5-inch
0	295.00	295.00	295.00	31	380.69	380.18	377.99
1	306.76	306.72	306.64	32	380.83	380.33	378.15
2	317.38	317.28	317.10	33	380.95	380.46	378.29
3	326.62	326.45	326.13	34	381.07	380.58	378.42
4	334.56	334.30	333.82	35	381.18	380.69	378.55
5	341.35	341.00	340.33	36	381.27	380.80	378.66
6	347.13	346.71	345.84	37	381.36	380.89	378.76
7	352.06	351.57	350.51	38	381.44	380.97	378.86
8	356.26	355.72	354.49	39	381.52	381.05	378.95
9	359.84	359.26	357.86	40	381.60	381.12	379.04
10	362.90	362.27	360.74	41	381.66	381.20	379.12
11	365.51	364.86	363.20	42	381.72	381.27	379.20
12	367.74	367.08	365.30	43	381.78	381.33	379.27
13	369.65	368.97	367.10	44	381.83	381.39	379.34
14	371.29	370.60	368.65	45	381.88	381.46	379.41
15	372.70	372.00	369.98	46	381.93	381.52	379.47
16	373.89	373.20	371.13	47	381.97	381.58	379.54
17	374.92	374.24	372.12	48	382.02	381.62	379.60
18	375.82	375.12	372.98	49	382.07	381.68	379.65
19	376.58	375.89	373.73	50	382.11	381.72	379.71
20	377.25	376.54	374.38	51	382.16	381.77	379.77
21	377.81	377.12	374.95	52	382.21	381.82	379.82
22	378.30	377.63	375.44	53	382.26	381.87	379.88
23	378.73	378.07	375.88	54	382.31	381.92	379.93
24	379.10	378.45	376.26	55	382.36	381.96	379.98
25	379.41	378.78	376.60	56	382.41	382.00	380.04
26	379.69	379.09	376.90	57	382.45	382.04	380.09
27	379.94	379.35	377.17	58	382.49	382.08	380.14
28	380.16	379.60	377.41	59	382.53	382.12	380.19
29	380.36	379.82	377.62	60	382.56	382.17	380.23
30	380.53	380.01	377.81				

CHAPTER 9

CONCLUSIONS AND FUTURE DIRECTIONS

In this research, a temperature distribution model for silicon wafer has been presented. Heat transfer theory is studied to understand the simulation method. Properties of silicon have been discussed in relation to the input to the model. Different meshing elements in each model has been considered to analyze the balance between efficiency and accuracy. A significant factor, thermal contact resistance, has been introduced to accomplish the model so that the simulated results could be in accord with the experimental data. After establishing the model, different values of wafer thicknesses and diameters were input to the model, and the results matched the theory.

For future directions, several reach areas could be explored. For semiconductor manufacturing processes, a more complicated model could be built. For example, the heating process for a silicon wafer, heated by RTP system, can be simulated if the required information is considered such as the design of the machine, energy value of the lamp etc. On a smaller scale, IC chips can be modeled to simulate the heat flow. Therefore, the status of the chip while heating can be studied to understand the influence of the heating process on the performance of the chips, which is useful in device reliability, develop a new process or material application[26]. Moreover, ANSYS can be used to simulate the carbon nanotube structure, as well as other 2-D structures - for example, the mechanical modeling of a single-walled carbon nanotube[27]. A variety of manufacturing and device applications can be considered.

References

[1] *AZ P4000 ® Thick Film Photoresist Data Sheet.*

[2] *SU-8 2000 Permanent Epoxy Negative Photoresist PROCESSING GUIDELINES.*

[3] Duerinckx, F. and Szlufcik, J., *Defect passivation of industrial multicrystalline solar cells based on PECVD silicon nitride.* Solar Energy Materials and Solar Cells, 2002. **72**(1): p. 231-246.

[4] Creighton, J.R., et al., *Emissivity-correcting mid-infrared pyrometry for group-III nitride MOCVD temperature measurement and control.* Journal of Crystal Growth, 2008. **310**(6): p. 1062-1068.

[5] Greiner, M.E. and Gibbons, J.F., *Diffusion of silicon in gallium arsenide using rapid thermal processing: Experiment and model.* Applied Physics Letters, 1984. **44**(8): p. 750.

[6] Bergman, T.L., DeWitt, D.P., Incropera, F.P, Lavine, A.S., *Fundamentals of heat and mass transfer*. 2011: John Wiley & Sons.

[7] Keshwani, M.P, Sheth, N.R., and Vyas, B.G., *Review: thermal contact resistance of metallic composite pair.* International journal of application or Innovation in Engineering & Management, 2015. **4**: p. 193-200.

[8] Kakac, S., and Yüncü, H., *Thermal contact conductance-theory and applications*, in *Cooling of Electronic Systems*. 1994, Springer. p. 677-702.

[9] Hummel, R.E., *Electronic properties of materials*. 2011: Springer Science & Business Media.

[10] Serway, R.A., Moses, C.J., and Moyer, C.A., *Modern physics*. 2004: Cengage Learning.

[11] Howell, J.R., Menguc, M.P., and Siegel, R., *Thermal radiation heat transfer*. 2010: CRC press.

[12] Zhu, X., et al., *The Effect of Mg Adding Order on the Liquid Structure and Solidified Microstructure of the Al-Si-Mg-P Alloy: An Experiment and ab Initio Study.* Metals, 2014. **5**(1): p. 40-51.

[13] Sze, S. M., & Ng, K. K. (2006). *Physics of semiconductor devices*. John wiley & sons.

[14] Föll, H., Langa, S., Carstensen, J., Christophersen, M., & Tiginyanu, I. M. (2003). Pores in III–V semiconductors. *Advanced Materials*, *15*(3), 183-198.

[15] Hull, R., *Properties of crystalline silicon*. 1999: IET.

[16] Sapoval, B., Hermann, C., & Hermann, C. (2003). *Physics of semiconductors*. Springer Science & Business Media.

[17] Shanks, H., et al., *Thermal conductivity of silicon from 300 to 1400 K.* Physical Review, 1963. **130**(5): p. 1743.

[18] Cverna, F., *Thermal properties of metals.* ASM International, Materials Park, OH, 2002.

[19] Middelmann, T., Walkov, A., Bartl, G., & Schödel, R. (2015). Thermal expansion coefficient of single-crystal silicon from 7 K to 293 K. *Physical Review B*, *92*(17), 174113.

[20] ASM International. Handbook Committee. (2004). *ASM handbook* (Vol. 9). G. F. Vander Voort (Ed.). Materials Park, OH: Asm International.

[21] Hughes, T.A., *Measurement and Control Basics*. 2002: ISA-The Instrumentation, Systems, and Automation Society.

[22] Baharav, Y., Ish-Shalom, Y., Jackson, G., *The use of temperature monitoring in advanced semiconductor industry processing.*

[23] Szafron, C., *Application of thermal imaging in electrical equipment examination.* Available: zet10. ipee. pwr. wroc. pl/record/181/files/39. pdf, 2008.

[24] Komarov, P.-L.,Burzo M. G., and Raad, P.-E., *CCD thermoreflectance thermography system: methodology and experimental validation.* arXiv preprint arXiv:0709.1854, 2007.

[25] Raad, P. E., Komarov, P. L., & Burzo, M. G. (2008). Thermo-reflectance thermography for submicron temperature measurements. *Electronics Cooling*, *14*.

[26] Nassiopoulou, A. G., & Kaltsas, G. (2000). Porous silicon as an effective material for thermal isolation on bulk crystalline silicon. *PHYSICA STATUS SOLIDI A APPLIED RESEARCH*, *182*(1), 307-312.

[27] Brostow, W., Castano, V.M., and Rangel, J.H., *Mechanical modeling of a single-walled carbon nanotube using the finite element approach.* Polimery, 2013. **58**(4): p. 276-281.